DEPARTMENT OF CHEMISTRY

NOVA SCHOOL OF SCIENCE & TECHNOLOGY

Tomás Alves Martins

# Biogas upgrading using supported liquid membranes with deep eutectic systems and carbonic anhydrase enzyme

MASTERS IN CHEMICAL AND BIOCHEMICAL ENGINEERING

NOVA SCHOOL OF SCIENCE AND TECHNOLOGY

April, 2024

DEPARTAMENT OF CHEMISTRY

# Biogas upgrading using supported liquid membranes with deep eutectic systems and carbonic anhydrase enzyme

**TOMÁS ALVES MARTINS**

**Advisers:** Luísa Alexandra Graça Neves
Assistant Researcher, NOVA School of Science and Technology
Rita Paula Paiva Craveiro,
Post Doctoral Researcher, NOVA School of Science and Technology

**Jury:**

**President:** Mário Fernando José Eusébio,
Assistant Professor, NOVA School of Science and Technology

**Member:** José Manuel da Silva Simões Esperança,
Principal Investigator, LAQV requimte

**Member:** Luísa Alexandra Graça Neves
Assistant Researcher, NOVA School of Science and Technology

MASTERS IN CHEMICAL AND BIOCHEMICAL ENGINEERING

NOVA School of Science and Technology
APRIL, 2024

**Biogas upgrading using supported liquid membranes with deep eutectic systems and carbonic anhydrase enzyme**

Dedicatory lorem ipsum.

# ACKNOWLEDGEMENTS

This work would not have been possible without the assistance of many people, for whom I am sincerely grateful.

To my supervisors Doctors Rita Craveiro and Luísa Neves for all the help provided during this work and during the many challenges that had to be overcome in order to have a successful work.

To all the people in the DES work group who helped me, made me laugh and feel integrated during this 1-year period of work.

To all my friends and family that provided love and help during this challenge, especially to one of my best friends, my grandfather whose one of his big dreams expressed to me since my childhood was to see me graduate and as an engineer. I know that he would be the happiest person in the world in this moment, and I know he would be proud. This thesis is also dedicated to him, as during this period, values like persistence, work ethic and above all the never give up attitude taught to me by him and the rest of my family since an early age were crucial for the success of this work.

"Good, better, best. Never let it rest. Until your good is better and your better is best"

(Tim Duncan)

# RESUMO

A aplicação de novas tecnologias sustentáveis para processos de purificação de biogás desempenhará um papel fundamental não só no presente, mas também nas próximas décadas. Solventes Eutécticos (DES) têm sido considerados uma alternativa promissora para processos de captura de $CO_2$ quando comparados aos solventes tradicionalmente usados, nomeadamente as soluções aquosas de aminas. Nesta tese, foram preparados 4 DES diferentes (cloreto de colina:ácido malónico (1:1), ácido lático:l-prolina:água (1:1:1), l-prolina:glicerol (1:2.5) e cloreto de colina:ácido lático (1:2)) e foram pré-equilibrados a diferentes valores de atividade de água ($a_w$) (entre 11.2 e 84.3%). Posteriormente, os DES foram caracterizados por FTIR, e a sua viscosidade, densidade, coeficiente de difusão do $CO_2$ e constante de Henry para o $CO_2$, foram determinadas. A enzima anidrase carbónica (AC), enzima que tem a capacidade de catalisar a reacção de conversão de $CO_2$ em bicarbonato, foi adicionada na concentração de 1 mg/g DES aos DES para avaliar o seu impacto no transporte de $CO_2$. O DES l-Prolina-glicerol com uma $a_w$ de 0.112 apresentou os melhores resultados apresentando o maior coeficiente de difusão de $CO_2$ dentro dos DES testados e com menor valor de constante de Henry. Por último, foram preparadas membranas líquidas suportadas (SLM) utilizando um suporte poroso hidrofílico de PTFE impregnado com o DES L-Prolina-Glicerol pré-equilibrado a $a_w$=0.112. Foram realizados ensaios de permeabilidade de gases para $CH_4$ e $CO_2$ a uma temperatura de 30ºC e pressão de 1 bar. A seletividade ideal e a permeabilidade foram calculadas e os resultados foram comparados com a literatura. A membrana líquida suportada preparada neste trabalho apresentou maior valor de permeabilidade ao $CO_2$ quando comparado com a literatura, no entando com uma selectividade ideial mais baixa ficando o seu valor abaixo do limite superior de Robson. Isto prova que novas estratégias devem ser implementadas em trabalhos futuros para aumentar a seletividade destas membranas impregnadas com Glicerol:L-Prolina.

**Palavras chave:** *Purificação de Biogás*, *Sistemas Eutécticos*, Anidrase Carbónica, Membranas Líquidas Suportadas

# ABSTRACT

The application of new sustainable technologies for biogas upgrading processes will have a key role not only in the present but also in the next few decades. Deep eutectic systems (DES) have been found to be a promising alternative for $CO_2$ capture processes when compared to the most commonly used - aqueous amine solutions. In this thesis, 4 different DES were prepared (choline chloride:malonic acid (1:1), lactic acid:L-proline:water (1:1:1), l-proline:glycerol (1:2.5) and choline chloride:lactic acid (1:2)) and were pre-equilibrated in different water activity values ($a_w$) (between 11.2 and 84.3%). Afterwards, the DES were characterized by FTIR, and their viscosity, density, $CO_2$ diffusion coefficient and Henry's constant were determined. Carbonic Anydrase, an enzyme that has the ability to catalyze the reaction of conversion of $CO_2$ to bicarbonate, was added in a concentration of 1 mg/g DES to the DES to evaluate its impact in $CO_2$ transport. L-Proline-glycerol (1:2.5) conditioned in the $a_w$=0.112 showed the best results having the highest diffusion coefficient within the group of DES tested and the lowest Henry's constant. Lastly, a supported liquid membrane (SLM) was prepared using a PTFE hydrophilic porous support impregnated with L-Proline-Glycerol pre-equilibrated at the aw=0.112. Gas permeability experiments were carried out for $CH_4$ and $CO_2$ at a temperature of 30ºC and pressure of 1 bar. The ideal selectivity and pure gas permeability were calculated, and the results were compared with literature. The SLM prepared in this work presented a higher $CO_2$ permeability value when compared to the other SLM using different DES and a lower selectivity, with its value falling below the Robson upper bound. This proves that new strategies need to be implemented in future works to increase selectivity of these membranes impregnated with Gly:L-Pro.

**Keywords**: Biogas Upgrading, Deep Eutectic Systems, Carbonic Anhydrase, Supported Liquid Membranes

# TABLE OF CONTENTS

# FIGURE INDEX

# TABLE INDEX

# ACRONYMS

| | |
|---|---|
| **$a_w$** | Water Activity |
| **ChCl** | Choline Chloride |
| **DES** | Deep Eutectic Solvents |
| **EU** | European Union |
| **Gly** | Glycerol |
| **HBA** | Hydrogen Bond Acceptor |
| **HBD** | Hydrogen Bond Donor |
| **ILs** | Ionic liquids |
| **LA** | Lactic Acid |
| **L-Pro** | L-Proline |
| **MA** | Malonic Acid |
| **PFTE** | Polytetrafluoroethylene |
| **SLMs** | Supported Liquid Membranes |
| **W** | Water |

# SYMBOLS AND VARIABLES

| | |
|---|---|
| **D** | Diffusion coefficient ($cm^2.s^{-1}$) |
| **ρ** | Density ($g.cm^{-3}$) |
| **H** | Henry's constant |
| **R** | Ideal gas constant ($cm^3.bar.K^{-1}.mol^{-1}$) |
| **P** | Pressure(bar) |
| **p** | Permeability (Barrer) |
| **L** | Solvent film height (cm) |
| **$\alpha$** | Selectivity |
| **T** | Temperature (Kelvin) |
| **t** | Time (s) |
| **μ** | Viscosity (mPa.s) |
| **V** | Volume ($cm^3$) |

# 1 Background, motivation and Dissertation Outline

In the present work the use of membrane separation processes using deep eutectic systems (DES) for biogas upgrading is studied. For many years, aqueous amine solutions have been used as the benchmark solvents for $CO_2$ absorption processes. However, in recent years several works have been reported in which deep eutectic systems have been presented as a more sustainable and biodegradable alternative to the more traditional solvents. This work considers the study of supported liquid membranes, combined with deep eutectic systems and an enzyme (carbonic anhydrase), and their possible use for biogas upgrading processes.

## 1.1 Background and Motivation

Adopted in 2015, the Paris Agreement was a historic global accord that aimed to reduce greenhouse gas emissions on developed countries[1]. It raised awareness of the pressing need for sustainability in several fields, including the generation of energy. Considering this, the search for alternative clean energy sources began. Biogas emerged as one of the promising alternatives to address the global challenges of waste management, energy security and environmental sustainability. Derived from organic matter through a natural biological process known as anaerobic digestion, this biofuel offers a clean and renewable alternative to traditional fossil fuels[2]. During this microbial process, bacteria break down the organic matter in the absence of oxygen, releasing a mixture of gases, with methane ($CH_4$) (50-70%) being the primary component. The composition of biogas also includes carbon dioxide ($CO_2$) (30-40%), traces of hydrogen sulfide ($H_2S$), and small amounts of other gases[3]. At the end of the anaerobic digestion process, the biogas produced usually needs go through an optimization process to increase its methane concentration (from 50-70% up to around 95%-99%) by reducing $CO_2$ concentration and achieve biomethane quality (defined as biogas upgrading) before being used as an energy source[4]. In recent years, strong efforts have been made to investigate and find sustainable biogas upgrading processes, in which chemical absorption based in different classes of solvents with affinity to capture $CO_2$ from a biogas stream and membrane absorption

have been looked at as promising alternatives. Aqueous amine solutions were the first class of solvents used in the $CO_2$ capture process industrially and are still the most used alternative to this day, but disadvantages such as poor sustainability, instability and high regeneration energy requirements make it crucial to look for new reliable and more sustainable options[5]. Consequently, ionic liquids (ILs), salts with melting point points below 100ºC, were considered possible replacements, since they possess advantages in comparison to amine solutions, such as low vapor pressure, high solubilization capacity and high chemical stability. Although ILs represent an improvement in $CO_2$ capture, their use also presents disadvantages since their synthesis is usually made from non-renewable raw materials and involves several steps, making their production expensive. Some ILs can also present toxicity issues, making them an unsuitable choice for industrial applications[6]. Therefore, there was an impending need to find a new type of solvent, which was a more sustainable option to ILs, that could be used as an $CO_2$ absorption solvent. Deep eutectic solvents (DES) are solvents that are usually formed by combining two or more compounds at a certain molar ratio—a hydrogen bond acceptor (HBA) and a hydrogen bond donor (HBD)— resulting in a complex hydrogen bonded network and a liquid mixture[7]. In recent years, DES potential as $CO_2$ absorbents has been explored by different authors[5], [8], [9], [10], [11] , and while the results were still lower than those of aqueous amine solutions, their performance was comparable to ILs, making them a promising alternative for $CO_2$ separation [5]. Besides gas absorption, other technologies have been presented and explored in recent years as the use of membrane technology for $CO_2$ absorption, using supported liquid membranes (SLMs) that are a non-dispersive liquid membrane system where a liquid absorbent occupies the pores of a microporous membrane[12]. Both ILs and DES have been used in combination with in SLMs, for biogas upgrading. In the research done during this thesis it was noticed that already multiple investigations have been done studying the potential of combining DES $CO_2$ capture capacity with supported liquid membranes, which motivated the theme of this thesis and the work developed during its duration period, of studying the viability of using different DES in supported liquid membranes as a biogas upgrading technique.

## 1.2 Dissertation Outline

This dissertation presents the work performed during this master's thesis and is organized in five chapters.

Chapter 1 includes the background, motivation and outline of this dissertation,

The second chapter includes the state of the art for biogas and biomethane in the current European context and the technologies used for biogas upgrading, in which the major technologies are described, with a particular focus on chemical absorption and 3 different classes of solvents: aqueous amine solutions, ionic liquids and deep eutectic systems. The enzyme carbonic anhydrase is also described, and the use of supported liquid membranes, a membrane separation technology which has been studied in recent years for gas separation. The third chapter describes the materials and methodology used during this work and the results obtained from DES physicochemical characterization and permeability tests are presented and discussed in Chapter 4.

In Chapter 5, the conclusions and future work are presented and discussed.

# 2 STATE OF ART

## 2.1 Biogas

Biogas is a gas naturally generated by the decomposition of organic matter (from plants or animal nature), done by bacteria in an oxygen free environment in a process called anaerobic digestion. Biogas production systems use anaerobic digestion to recycle organic matter, transforming it into biogas, which contains high energetic value and other valuable products associated with soil treatment (solids and liquids), as shown in Figure 2.1 [13].

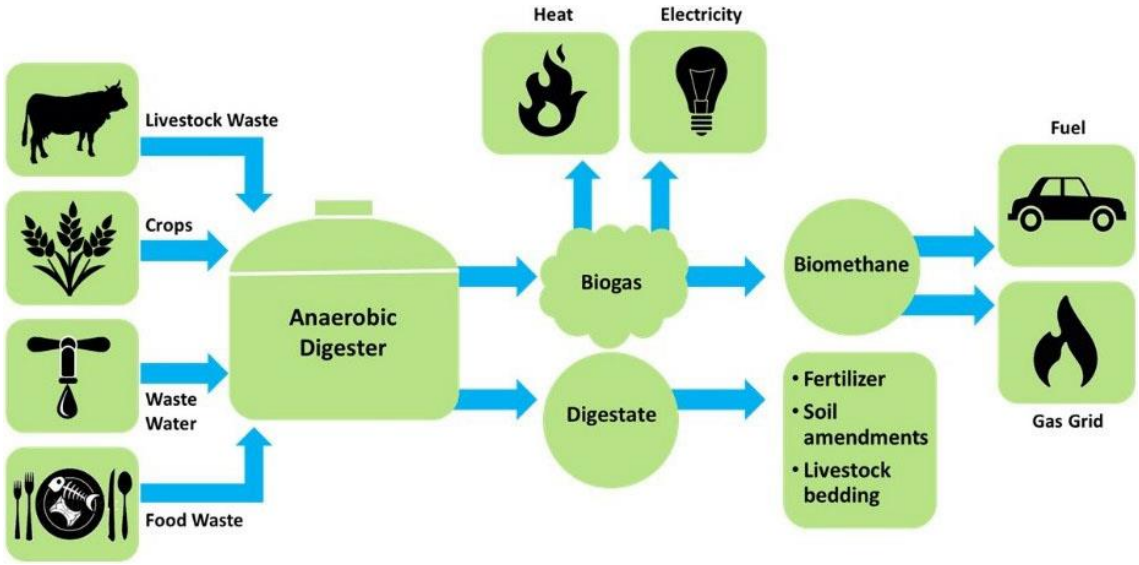


Figure 2.1-Biogas production and products. (adapted from fact sheet|Biogas:Converting waste to Energy)[13]

The biogas production process begins with the processing/pre-treatment of the organic matter (biomass), before feeding it to the reactor where the anaerobic digestion process will take place, followed by a purification step which is essential to guarantee the quality of the biogas produced and thus minimize possible risks during its use. Once this stage is completed, the anaerobic digestion process begins, which is a chemical process that can be summarized in 4 phases:

- **Hydrolysis**- phase in which long-chain polymers such as cellulose are hydrolyzed and transformed into products such as glucose;

- **Acidogenesis and Acetogenesis**-phases characterized by the production of gases, more specifically hydrogen and carbon dioxide from glucose and other monomers;
- **Methanogenesis**- the last phase, in which most of the methane ($CH_4$) is produced [14].

Raw biogas composition is influenced by the nature of biomass used during this process. Generally, at the end of this process, biogas is mostly composed of carbon dioxide ($CO_2$) (30-40%) and methane ($CH_4$) (50-70%), while also containing residual amounts of nitrogen ($N_2$), hydrogen ($H_2$), hydrogen sulfide($H_2S$), water ($H_2O$), ammonia ($NH_3$) and carbon monoxide (CO) [15].The presence of $CO_2$ and impurities in the composition of biogas, reduces its energetic power. For this reason, it is necessary to separate $CO_2$ from methane, to obtain pure biogas-biogas upgrading- before biogas is used as energy source [14].

### 2.1.1 Context in the European Union

Since the formation of the European Union (EU) in 1993, the topic of environmental awareness had always a prominent place in the policies and objectives outlined by the European union, both collectively and individually, with regards to each of its member states. These environmental policies were introduced almost 20 years later, in accordance with the growing concern associated with the increase in global warming levels, making it one of the most discussed topics still today, the climate change [16].

In line with this trend, all participants in the Paris Agreement signed in 2015 by 190 countries (including all EU member states) committed to reduce their emissions to limit the increase in global average temperature to less than 2$^{o}$C, preferably less than 1.5$^{o}$C [17], compared to pre-industrial levels, to mitigate the risks and impacts of climate change.

To achieve this goal, the EU decided to intensify greenhouse gas emission-reduction measures, and more recently in 2020, a new agreement called The Green Deal was implemented, in which it is established that a reduction of gas emissions of 55% should occur by 2030, compared to 1990 gas emission levels[17].

On the other hand, other measures were addressed by the EU to promote the path towards carbon neutrality, assumed as a goal to be achieved in the year 2050, among promoting the use of energy obtained from renewable energy sources, in which a minimum consumption

target of 32% from renewable energy was established in terms of total energy consumption, thus seeking to increase energy independence from non-renewable sources, such as fossil fuels[16].

Within this framework, biogas and biomethane are positioned as promising alternatives in the sustainable energy transition, providing an alternative energy source [16].

The combined production of these two biofuels in 2021 accounted to 18.4 billion cubic meters (bcm) (as shown in Figure 2.2), representing 4.5 % of the European Union's Gas consumption of that year. While biomethane production continues to grow, the same cannot be said about biogas production, as 2021 witnessed the largest annual increase, with a 20% growth compared to 2020[18].

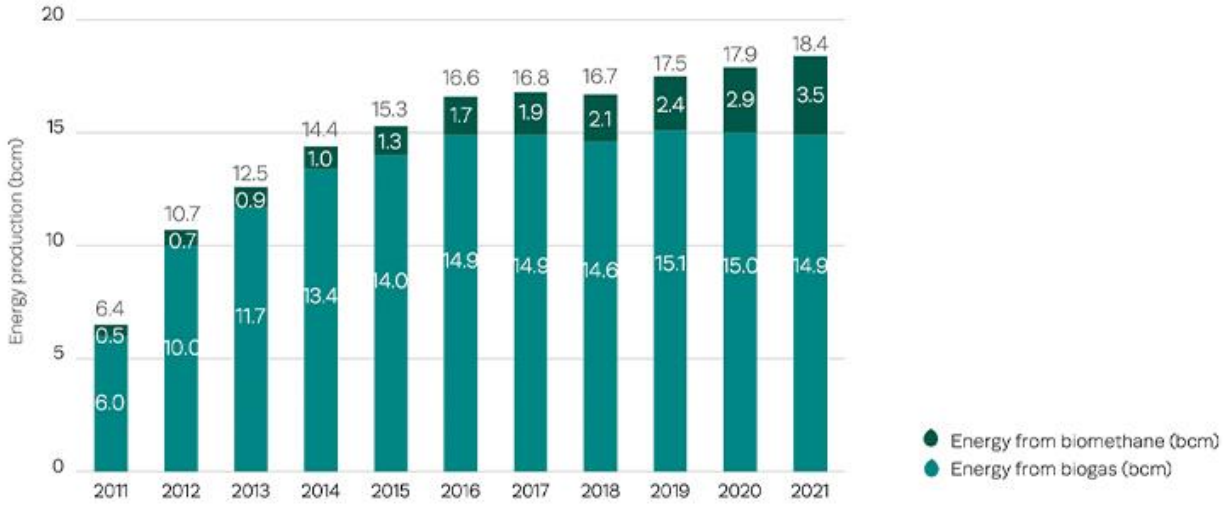


Figure 2.2-Biogas and Biomethane Production in Europe between 2011-2021. (adapted from EBA 2021)[18]

As can be seen in Figure 2.3, there has been a substantial growth in the number of biomethane plants since 2011 until 2022, which meets the current and future European energetic needs and targets. In 2022, as shown in Figure 2.3 there were 1222 biomethane plants in Europe and in the last 3 years there was the largest increase in the number of biomethane plants until the present date[19], reinforcing the growth in demand of this biofuel.

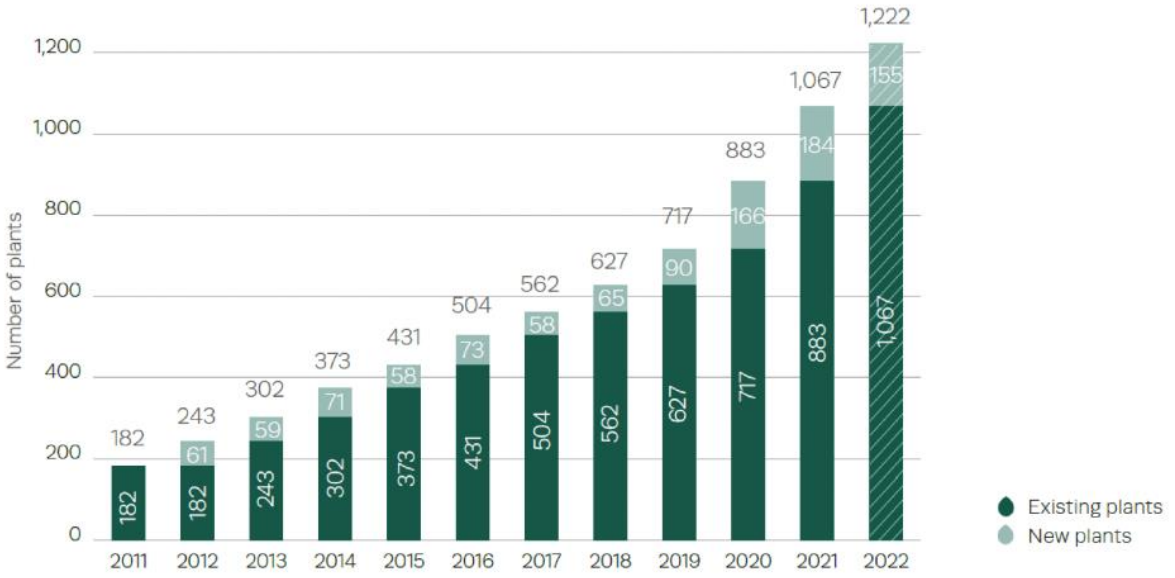


Figure 2.3-Evolution of Biomethane plants in Europe. (Adapted from Development of the European biogas and biomethane production market-EBA statistics 2022)[20]

Furthermore, with the pressing need of decreasing current dependency on Russian natural gas underlined in the REPowerEUPlan, a plan proposed by the European Commission that seeks to cut the European Union's reliance on Russian fossil resources as quickly as possible published in May 2022, present and future growth in biomethane production becomes one of the key solutions to increase European energy security and should be expected in the next few years, having a target of 35 bcm for biomethane production by 2030, compared to todays 3.8 bcm of biomethane (Figure 2.4) and 15 bcm of biogas produced in the EU-27[19].

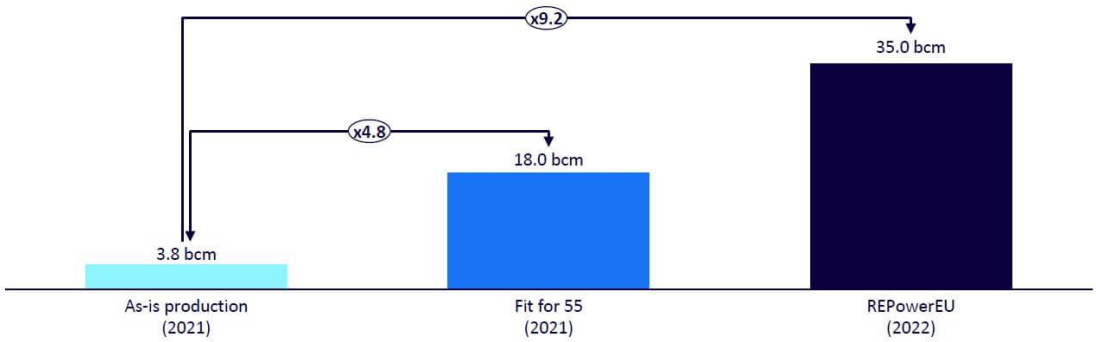


Figure 2.4- Comparing current and EU 2030 biomethane production targets(Adapted from Arthur D. Little, EBA, EU regulation)[20].

According to the current projections (Figure 2.5), biomethane production is expected to grow in the EU, but fall short of the 35 bcm target[20]. It is important to invest and develop new technologies that make biogas upgrading process a greener and economically feasible one, while providing the necessary rate of $CO_2$ purification, for good biomethane quality.

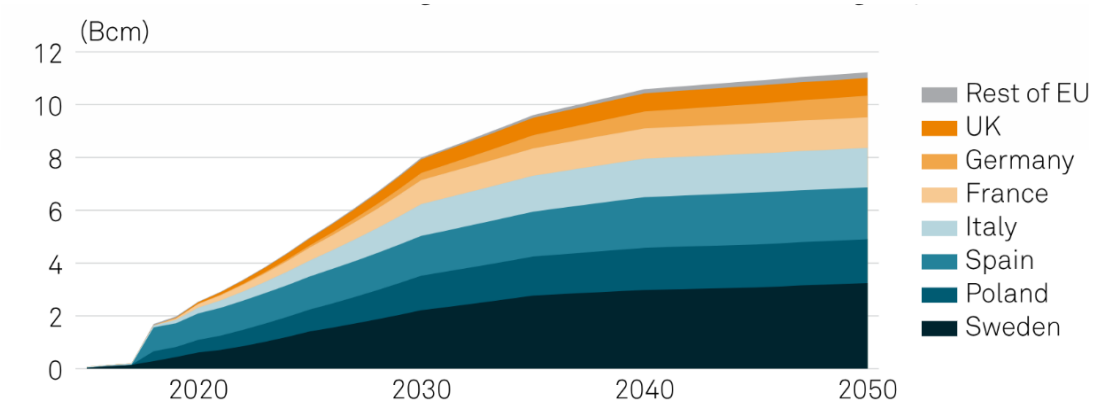


Figure 2.5- EU Biomethane Production Projection until 2050.(Adapted from Development of the Biomethane Market in Europe)[20]

## 2.2 Biogas upgrading

As mentioned before, the biogas produced from anaerobic digestion can be used as a renewable source of energy. According to its final application, its purification is often necessary, namely the removal of carbon dioxide ($CO_2$) and hydrogen sulfide ($H_2S$)[15] [2]. Therefore, the final objective of the "upgrade"/purification process is to optimize the concentration of biomethane ($CH_4$) up to 95-99% of the total biogas composition, in order to maximize the calorific

value of this biofuel, so that it can be used as an efficient fuel and also to be incorporated into the natural gas energy networks that feed different industries and homes [21].

Using the right technology, it becomes feasible to replace fossil fuels normally used as Compressed Natural Gas (CNG) or Liquefied Natural Gas (LNG) with an equivalent biofuel. The biomethane obtained from biogas upgrading can be liquified (Bio-LNG) or compressed (Bio-CNG) to be used as vehicle fuel (Bio-VNG), as one of its main applications. Furthermore, when in comparison to fossil fuels, biomethane allows a similar engine performance, being a suitable and greener choice[17].

When considering biogas purification to biomethane, mainly $CO_2$ separation, membrane separation is now the most extensively utilized technology (39%), followed by water scrubbing (22%) and chemical absorption (18%). Other technologies are used, such as pressure swing adsorption (12%), cryogenic separation (1%), and physical washing (1%), except for 7% of European biomethane facilities, for which there is no data in the European Biogas Association (EBA) database (Figure 2.6)[22].

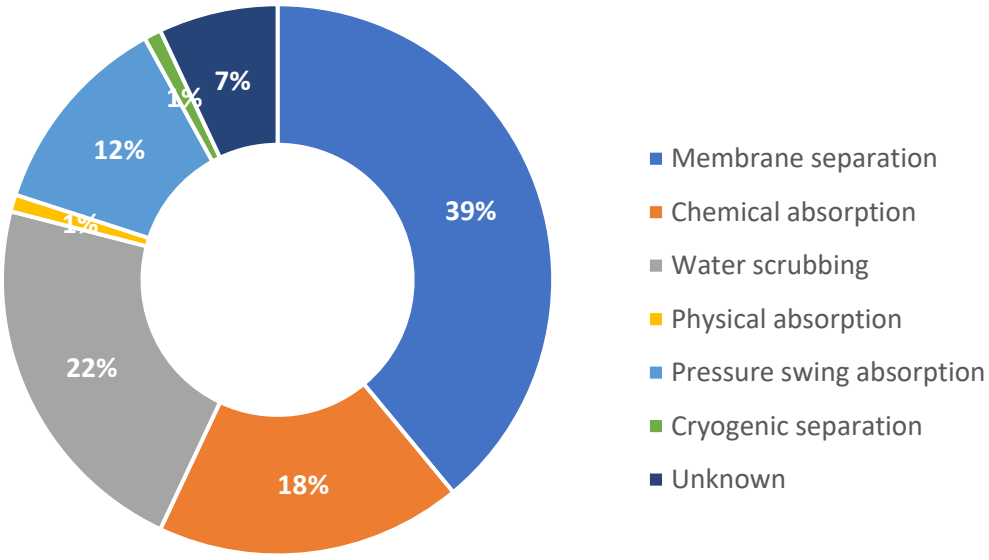


Figure 2.6- Market share of different upgrading technologies in Europe in 2020.(Adapted Recent Advances in Membrane-Based Biogas and Biohydrogen Upgrading)[22]

Pressure swing adsorption (PSA) is a physical adsorption technology known for being very versatile in the field of separation and purification of gas mixtures. In PSA processes, a

pressurized biogas stream is fed to a column where it contacts with an adsorbent (normally a porous solid with a high surface area) that will selectively adsorb $CO_2$. Afterwards, the purified biogas stream exits at the top of the column, and the adsorbent which is saturated with $CO_2$ is regenerated by reducing operating pressure (normally to vacuum)[23].

Physical absorption is an upgrading technology based on absorption process without chemical reaction where biogas enters in a packed column in the bottom and the liquid absorbent is sprayed from the top of a packed column filled with packing materials that help increase the $CO_2$ mass transfer area in a counterflow mode. The purified biogas is then collected at the top while the stream with absorbed $CO_2$ is obtained at the bottom of the column[24].

Water scrubbing is a process based on physical absorption in which water is used as a solvent to solubilize $CO_2$. This method is used due to the higher solubility of $CO_2$ in water than $CH_4$ and is carried out using a packed column, where biogas is introduced at high pressure at the bottom of the absorption column while a water stream enters at the top and flows down inside the column, providing mass transfer of $CO_2$ from the biogas in counterflow mode, similarly, to previously described. Consequently, the purified biogas stream (biomethane) exits the column at the top, and the water stream with dissolved $CO_2$ is let out at the bottom being then redirected to a regeneration column where after most of the absorbed $CO_2$ is removed from water, and the $CO_2$-less stream is reutilized in the absorption system [24].

On the other hand, chemical absorption process is the process used industrially to capture $CO_2$. In this process, the reaction of $CO_2$ with a solvent takes place, to form a weakly bound intermediate compound that can be regenerated by heating to obtain the original solvent and a separated stream of $CO_2$ [25]. Three main solvents have mainly been studied for this type of process: aqueous amine solutions, ionic liquids (ILs) and most recently deep eutectic systems (DES). The $CO_2$ chemical absorption process using aqueous amine solutions as solvents, is the most used process for $CO_2$ removal at industrial scale. Several types of amines have been tested over the years including monoethanolamine (MEA) a primary amine; diethanolamine (DEA) a secondary amine, and methyldiethanolamine (MDEA) a tertiary amine, which are the most used in the absorption process. In the case of primary and secondary amines, they have a high reaction rate during the absorption of $CO_2$, which begins with the formation of a zwitterion (Equation 2.1), which then transfers a proton to an amine giving rise to the formation of carbamate (Equation 2.2). The carbamate ion can then be hydrolyzed at high pressures to regenerate the free amine and bicarbonate, as the amine is in that moment available to react again with $CO_2$(Equation 2.3)[26]

$$R_1R_2NH + CO_2(aq) \leftrightarrow R_1R_2NH^+COO^-$$ (Equation 2.1)

$$R_1R_2NH + R_1R_2NH^+COO^- \leftrightarrow R_1R_2NH^+ + R_1R_2NCOO^-$$ (Equation 2.2)

$$R_1R_2NCOO^- + H_2O \leftrightarrow R_1R_2NH + HCO_3^-$$ (Equation 2.3)

Primary and secondary amines show some limitations when it comes to absorbing $CO_2$ since it is only possible to load a maximum of 0.5 moles of $CO_2$/mole of amine. On the other hand, tertiary amines can absorb more $CO_2$ (1 mol $CO_2$/mol amine) while also needing less energy for their regeneration. However, the low reaction rate hinders their application when it comes to $CO_2$ absorption[26]. The use of these amine aqueous solutions has numerous disadvantages, and their use is limited by factors such as their reduced sustainability, limited number of cycles of absorption and desorption, high instability, volatility, toxicity, possibility of corrosion of equipment and the need for very high energy consumption for their regeneration[5]. Thus, there is the need to search for and develop more sustainable/greener alternatives that can replace these solvents, that are less prone to degradation and have high affinity for $CO_2$, highlighting in recent years, Ionic Liquids (ILs) and Deep Eutectic Systems (DES)[27].
Ionic Liquids (ILs) are a class of unconventional solvents, that have generated a growing interest in the last two decades, from different areas of research in the field of chemistry and have been presented as a viable alternative to solvents composed of amines, in terms of $CO_2$ absorption [28]. These compounds are salts, composed by cations and anions, which are liquid at temperatures below 100°C, including at room temperature. ILs are often defined as "designer solvents" since their intrinsic properties can be adjusted depending on their final application by simply replacing the combination of cations and/or anions in their structure. In addition, they have a high gas absorption capacity, low vapor pressure, thermal stability and easy regeneration which makes them extremely appealing to be used as absorbents for the capture of $CO_2$.[29][10]. On the other hand, the existence of major disadvantages, including the fact that they are synthesized from chemical reactions that use non-renewable products, which makes them expensive and limits their application in large-scale processes, as well as their

toxicity mainly towards aquatic organisms made it crucial to search for new solvents that could overcome the drawbacks of ILs[5].

DES are recognized as a possible viable alternative to replace ILs in $CO_2$ capture applications, as some of these solvents share many of their advantageous properties, including high thermal stability, low volatility, low vapor pressure, while also presenting benefits over the former, being typically cheaper, biodegradable, easier to prepare, not requiring any type of purification of the constituent components and not being toxic[30]. These solvents are prepared by mixing a hydrogen bond acceptor species (HBA) with a hydrogen bond donor species (HBD), that according to an adequate molar ratio and at a given temperature, establish a network of hydrogen bonds between them and form an eutectic liquid mixture[31] In DES there is a significant drop in the melting point compared to that of its individual components [11], as seen in Figure 2.7. This figure shows a two component phase diagram highlighting the formation of a eutectic mixture, that occurs due to the displacement of charge that takes place at the moment of formation of hydrogen bonds.

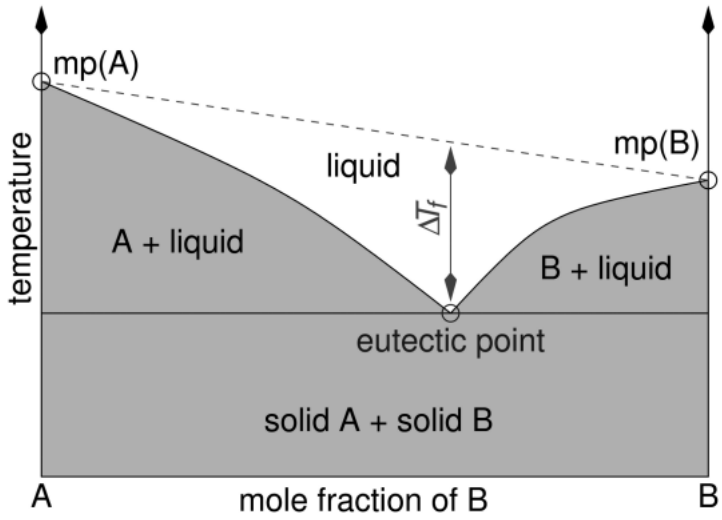


Figure 2.7-Two component solid-liquid phase equilibrium diagram.(Adapted from Eletrodeposition from Deep Eutectic Solvents)[10]

As mentioned before, the ability of DES to absorb and solubilize $CO_2$ has been a topic of interest in recent years, particularly towards the study of the use of a variety of these solvents as potential $CO_2$ separation/capture "agents", with promising results being obtained in some cases. These systems generally have lower $CO_2$ solubility than aqueous solutions of amines

and a $CO_2$ capacity comparable to that of ILs (for example, at 298 K and 10 bar, the $CO_2$ solubility in ChCl:TEG DES is equivalent to 2.0 wt%, whereas in aqueous 30% MEA it is 11.95 wt%). According to this fact, DES functionalized with amines were introduced to increase the capacity of $CO_2$ solubilization. Adeyemi *et al.* observed three distinct molar ratios of 1:6, 1:8, and 1:10 for ChCl-based DESs coupled with amines MEA, DEA, and methyldiethanolamine (MDEA). In comparison to a 30 wt% MEA solution, the solubility of $CO_2$ in amine-based DES was reported to be significantly higher (around 0.486 mol $CO_2$/mol ChCl-MEA 1:8 when compared to 0.144 mol $CO_2$/mol MEA)[32]. On the other hand, Leron *et al.* examined the solubility of $CO_2$ in Choline Chloride:glycerol (1:1) at 30 °C and 18.7 bar , and they obtained a value of 0.0163 mol $CO_2$ /mol ChCl-Gly. In another work, Craveiro *et al.* using the pressure decay method, determined the $CO_2$ solubility in different choline chloride based DES, namely choline chloride:glycerol (ChCl:GLY (1:2)), choline chloride:urea (ChCl:U(1:2)), choline chloride:ethyleneglycol (ChCl:EG(1:2)) and choline chloride:oxalic acid (ChCl:OA(1:2)). The values obtained were situated between 0.0055 and 0.006 mol $CO_2$/mol DES [5]. In addition, there are also some studies that have explored using amino acids-based DES in $CO_2$ sequestration. Ren *et al.* demonstrated that L-arginine:glycerol DES with mole ratios of 1:5, 1:6 and 1:7 showed a high absorption capacity of up to 0.511 mol $CO_2$/mol DES in a temperature range of 40-80$^{o}$C under atmospheric pressure [11].

With the growing interest in these solvents and with the objective of promoting recyclability and reusability in $CO_2$ sequestration processes, DES can be immobilized in a physical support such as supported liquid membranes [5]. Supported Liquid Membranes (SLMs) are non-dispersive liquid membranes where a solvent is immobilized inside the pores structure of a microporous support that can be either polymeric or ceramic, by capillary forces[12]. The membrane acts as a semi-permeable barrier between 2 phases, where $CO_2$ transport is governed by solution diffusion mechanism as the desired gas molecules (in this case $CO_2$) are absorbed in the SLM followed by their diffusion across the membrane and desorption on the permeate side[33]. Supported liquid membranes using DES as a solvent combine the advantages of membranes with the $CO_2$ capture capacity of some DES, while also preventing low performance results of the liquid membrane due to evaporation of solvent, since DES have negligible vapor pressure. When compared to other types of liquid membranes (bulk liquid membranes (BLMs) and emulsion liquid membranes (ELMs)), supported liquid membranes have several important benefits, including high permeability, high mass transfer rate, high extraction efficiency, high stability, and low cost[8]. Furthermore, while selective mass transfer is a

membrane's primary function in traditional membrane separation processes, the semipermeable membrane present in this type of liquid membrane serves only as a separation barrier to separate the gas and the absorbent, enhancing the surface area for mass transfer but does not provide any selectivity to separate the mixed gases present in the gas phase as mass transfer occurs due to the diffusion of components from one phase to the other as mentioned before, and selectivity is granted by the absorption liquid (solvent) with high affinity towards the target component ($CO_2$ in the case of this work) chosen according to the separation rate required[34].

Moreover, based on the composition and flow rate of feed gas, system operation needs, the ideal membrane materials for an efficient separation are chosen. Membranes are usually divided into polymeric and inorganic membranes although the first ones mentioned are preferred for $CO_2$ capture as they offer a wide range of advantages related to their lower manufacturing costs, ease of fabrication and physicochemical features than can be controlled considerably more easily than those of inorganic membranes. Furthermore, membrane materials need to be thermally and chemically compatible with the operating conditions and with the adsorbent used, and typically have a thickness ranging from 10 to 300 μm. The typical polymers used in supported liquid membranes are displayed in Table 2.1.

Table 2.1- Typical polymers used in supported liquid membranes. (adapted from [35])

| Polymer | Chemical Structure | Polymer | Chemical Structure |
|---|---|---|---|
| Polysulfone (PSF) | 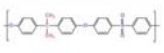 | Polypropylene (PP) |  |
| Polyethersulfone (PES) |  | Polyvinylidene (PVDF) |  |
| Polyether ether ketone (PEEK) | 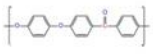 | Polytetrafluoroethylene (PTFE) |  |
| Polyetherimide (PEI) | 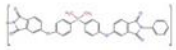 | Polymethyl pentene (PMP) |  |
| Polyethylene (PE) |  | Polydimethylsiloxane (PDMS) |  |

Among these hydrophobic polymers used in supported liquid membranes, polypropylene (PP), polytetrafluoroethylene (PTFE) and polyvinylidene fluoride (PVDF) are the most used membrane materials in gas absorption membrane systems. PP and PTFE provide excellent chemical stability, making them a desirable choice for membrane materials to be used in membrane operations[35][36].

Furthermore, the $CO_2$ capture process can also be improved based on biological systems with the help of an enzyme, more precisely carbonic anhydrase. Carbonic anhydrase enzyme has considerable potential to improve $CO_2$ absorption and desorption because of its extraordinarily high turnover number of $10^6$ $s^{-1}$, which is determined by the maximum number of substrate molecules transformed into product per active center and per unit of time when the enzyme is saturated and is one of the most essential properties of its enzymatic activity. This can enhance reaction kinetics and lower the energy costs associated with releasing absorbed $CO_2$ in solvent-based $CO_2$ capture methods[37]. Previous works have reported the use of this enzyme in supported liquid membranes with Ionic Liquids[38] and more recently with DES[5]. This group of enzymes are a group of metalloenzymes that exist in prokaryotic and eukaryotic organisms that are used in several industrial applications such as the capture of post- combustion $CO_2$ produced during the production of fossil fuels, in calcite production, a mineral which is used in agriculture and construction materials, and in biofuel production[39]. When it comes to biogas upgrading to biomethane, carbonic anhydrase acts as a catalyst in the reversible of $CO_2$ hydration reaction, in which bicarbonate is produced (Equation 2.4)[42].

$$CO_2 + H_2O \leftrightarrow H_2CO_3 \text{(Equation 2.4)}$$

Therefore, $CO_2$ membrane absorption can be enhanced by the presence of this enzyme because when carbonic anhydrase is present in the DES filling the membrane pores, $CO_2$ is constantly being transformed into bicarbonate ($H_2CO_3$). As bicarbonate diffuses through the supported liquid membrane, it then desorbs and is reconverted into $CO_2$ when a sweep gas or vacuum is used on the permeate side[5]. This extra enzymatic mechanism coupled with the affinity of DES for $CO_2$ is expected to improve the amount of $CO_2$ captured by the membrane process, due to simultaneous absorption and reaction mechanism. In addition, another advantage related to the use of this enzyme is that CA shows good selectivity for $CO_2$, which boosts the membrane's selectivity for this gas in comparison to other gases (in the case of this work $CH_4$), that is one of the crucial parameters when evaluating and ensuring the success of gas separation/capture processes[8]. When working with enzymes an important aspect to have in mind is guaranteeing the adequate conditions for enzyme solubilization, activity and stability. Taking this into consideration, hydrophilic DES were chosen for this work since water content is a key factor when it comes to enhancing the activity of the enzyme[40]. In a previous work, Craveiro *et al.* prepared four different choline chloride based DES (ChCl:U (1:2), ChCl:Gly

(1:2), ChCl:EG (1:2) and ChCL:OA (1:2)) and $CO_2$ solubility and diffusivity coefficients were assessed. Moreover, PTFE polymeric membranes were prepared and impregnated with the mentioned DES and the pure gas permeability was measured for various gases ($CH_4$, $CO_2$ and $N_2$), as well as the membrane's ideal selectivity[5]. These experiments were done in the presence and absence of CA to analyze the effect of this enzyme in $CO_2$ capture results. The results obtained showed that the supported liquid membrane made with ChCl:U DES was a viable $CO_2$ capture alternative, since it showed highest permeability and selectivity for $CO_2/CH_4$. The present work is based on the former , in which different hydrophilic DES were prepared (ChCl:MA (1:1), LA:L-Pro:W (1:1:1), L-Pro:Gly (1:2.5) and ChCl:LA (1:2)) with and without CA and were pre-equilibrated in 4 different water activities($a_w$) before being characterized (by FTIR, density, viscosity ,$CO_2$ diffusivity). $CO_2$ diffusion coefficient and Henry's constant values for the different DES, with and without the presence of CA, were determined. After the selection of the DES with the highest affinity towards $CO_2$, supported liquid membranes were prepared and gas permeability and ideal selectivity were determined.

# 3 MATERIALS AND METHODS

## 3.1 Materials

The reagents used in this work for DES preparation were choline chloride (CAS 67-48-1, Sigma Aldrich), L-Proline (CAS 147-85-3, Sigma-Aldrich), DL-Lactic acid (CAS 50-21-5, Sigma Aldrich), malonic acid (CAS 141-82-2, Sigma Aldrich), and glycerol (CAS 56-81-5, Sigma Aldrich) are listed in Table 3.1.

Table 3.1- List of reagents used for DES preparation, their molecular weight and purity(%).

| Reagent | Chemical Formula | Molecular Weight(g/mol) | Purity (%) |
|---|---|---|---|
| choline chloride | $[(CH_3)_3NCH_2CH_2OH]^+Cl^-$ | 139.62 | ≥98% |
| L-Proline | $C_5H_9NO_2$ | 115.13 | 99% |
| DL-lactic acid | $C_3H_6O_3$ | 90.08 | 88-92% |
| malonic acid | $C_3H_4O_4$ | 104.06 | 99% |
| glycerol | $C_3H_8O_3$ | 92.09 | ≥99.5% |

For the preparation of salt mixtures to create different water activity values, the salts used were lithium chloride (CAS 7447-41-8, Sigma Aldrich), potassium chloride (CAS 7447-40-7, Honeywell Fulka), magnesium nitrate hexahydrate (CAS 13446-18-9, Honeywell Fulka), and potassium acetate (CAS 127-08-2, Riedel-de Haen) are listed in Table 3.2.

Table 3.2- List of reagents used for salt solution preparation and salt solution water activity.

| Salt | Chemical Formula | Water activity ($a_w$) |
|---|---|---|
| lithium chloride | LiCl | 0.112 |
| potassium acetate | $CH_3COOK$ | 0.226 |
| magnesium nitrate hexahydrate | $Mg(NO_3)_2.6\ H_2O$ | 0.529 |
| potassium chloride | KCl | 0.843 |

The enzyme used was carbonic anhydrase (CA) from bovine erythrocytes from Sigma Aldrich (lyophilized powder, ≥2000 W-A units/mg protein). Polytetrafluoroethylene (PTFE) membranes with pore size of 0.2 μm were obtained from Merck Milipore and were used to prepare the supported liquid membranes (SLM). The gases used during solubility and permeation tests were carbon dioxide ($CO_2$, 99.998%), methane ($CH_4$, 99.99%) and Helium (He, 99.99%). All gases were supplied by Praxair.

## 3.2 Methods

### 3.2.1 DES preparation

The DES used during this thesis were prepared by weighing, mixing, and heating the components of the desired DES in the adequate molar ratio, until obtaining a homogeneous mixture as seen in Figure 3.1. Most of the DES prepared were heated to a temperature of 80ºC, with the exception being LA:L-Pro:W that was heated to a temperature of 40ºC to prevent L-Proline decomposition. After that, liquid mixtures were obtained. In the cases where there is the presence of CA, the enzyme was weighed and added to the DES, achieving the desired concentration. Table 3.3 shows the molar ratios and respective molecular weights of the prepared DES.

Table 3.3- Deep Eutectic Systems used in this thesis, with their molar ratio and molecular weight.

| Composition | DES name | Molar Ratio | Molecular Weight(g/mol) | Melting Point(ºC) | Concentration of CA (mgCA/gDES) |
|---|---|---|---|---|---|
| **L-Proline:Lactic Acid:Water** | L-Pro:LA:W | 1:1:1 | 74.41 | - | - |
| **L-Proline:Lactic Acid:Water with CA** | L-Pro:LA:W_CA | 1:1:1 | 74.41 | - | 1.0 |
| **L-Proline:Glycerol** | L-Pro:Gly | 1:2.5 | 98.67 | - | - |

| | | | | | |
|---|---|---|---|---|---|
| **L-Proline:Glycerol with CA** | L-Pro:Gly_CA | 1:2.5 | 98.67 | - | 1.0 |
| **Choline Chloride:Malonic Acid** | ChCl:MA | 1:1 | 121.61 | 10 | - |
| **Choline Chloride:Malonic Acid with CA** | ChCl:MA_CA | 1:1 | 121.61 | 10 | 1.0 |
| **Choline Chloride:Lactic Acid** | ChCl:LA | 1:2 | 106.44 | -63.99 | - |
| **Choline Chloride:Lactic Acid with CA** | ChCl:LA_CA | 1:2 | 106.44 | -63.99 | 1.0 |

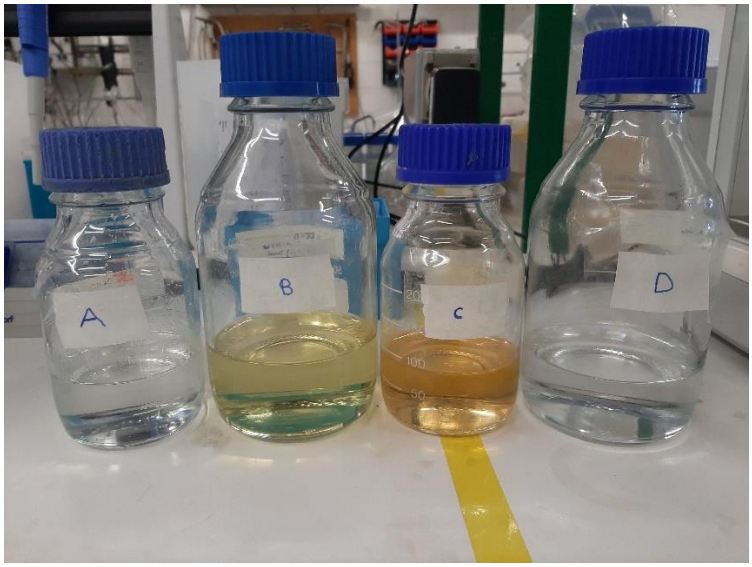


Figure 3.1- DES prepared in this work: A) Choline Chloride:Malonic Acid (1:1), B) L-Proline:Lactic Acid: Water (1:1:1),C) L-Proline:Glycerol (1:2.5), D) Chloine Chloride:Lactic Acid (1:2).

### 3.2.2 Saturated salt solutions preparation for DES conditioning

In this work, 4 different saturated salt solutions were prepared by weighing and slowly mixing the salt and water quantities in a desiccator as shown in Table 3.4. After obtaining the solutions, they were left to equilibrate for some time at 30ºC. DES samples, with and without CA were placed in each desiccator, at different $a_w$ values, until the water content of each sample remained constant, which was guaranteed by Karl-Fisher titration.

Table 3.4- List of salt solutions used for DES conditioning at different aw[41].

| **Solution** | **Salt Quantity (Kg)** | **Water Quantity (Kg)** | **Water Activity ($a_w$) at 30ºC** |
|---|---|---|---|
| Lithium Chloride | 0.075 | 0.042 | 0.112 |
| Potassium Acetate | 0.200 | 0.075 | 0.226 |
| Magnesium Nitrate Hexahydrate | 0.150 | 0.023 | 0.529 |
| Potassium Chloride | 0.200 | 0.080 | 0.843 |

## Physico-chemical Characterization

### 3.2.2.1 Water content determination

The Karl-Fischer titration method was used to determine the water amount in the prepared DES, with and without enzyme. In this work, an 831 KF coulometer (Metrohm) without diaphragm was used, using HYDRANAL- Coulomat AG (67-56-1) as anolyte. The results obtained throughout this work were derived from the average of at least three measurements per sample, carried out at room temperature.

### 3.2.2.2 Fourier Transform Infrared Spectroscopy (FTIR) – Attenuated Total Reflectance mode (ATR)

Due to high sensitivity, flexibility, and specificity, when it comes to detecting and measuring chemical substances in a sample, Fourier Transform Infrared Spectroscopy, or FTIR, is frequently used[42]. This method is based on the absorption of infrared light (IR) by a sample as it passes through it, altering the dipole moment of the sample molecules at particular wavelengths resulting in a spectrum. In FTIR spectra, the interactions of IR light with chemical functional groups results in bands that occur at defined wavelengths, allowing their identification[43].

In this work, the FTIR spectra of different samples were collected in the attenuated total reflectance (ATR) mode. This allows the analysis of samples (solid or liquid) using smaller quantities without the need for previous sample preparation.

This technique is based on the attenuations/changes that occur to an emitted infrared radiation beam that is totally reflected when it meets the sample. To do this, the infrared beam is focused at a certain angle on an ATR crystal (absorbing infrared radiation and with a high refractive index). The successive internal reflections create a wave that goes beyond the external surface of the crystal and penetrates the sample that is in contact with it. The wave produced initially is altered, and at wavelengths where the sample absorbs energy, the wave is altered or attenuated [44]. The resulting attenuated wave goes back to the inner surface of the crystal, is measured in the spectrometer's detector, and the system uses the data to generate a spectrum.

In this work, the FTIR spectra were obtained using a Pelkin Elmer FTIR Spectrum TwoTM spectrometer in transmittance mode, equipped with an ATR system, in a wavelength range of 400-4000 $cm^{-1}$.

## Rheology

The resistance of a medium under shear stress to progressive deformation is known as viscosity. Viscosity can depend on the shear strain-rate and time ("Non-Newtonian" fluid) or be independent ("Newtonian" or "ideal-viscous" fluid), but it also depends on temperature which has a huge impact on this physical property[45].

For DES characterization, viscosity measurements are important due to the influence this property can have on gas diffusion. Viscosity is also found to be highly dependent on the amount of water present in each DES[46].

The rheological measurements of the different DES equilibrated at different water activity values were made in an Anton Paar Modular Compact Rheometer Model MCR 102 and using the Rheocompass program by Anton Paar. Measurements were acquired within the temperature interval 20-80ºC. The rheometer geometry used in these measurements was a parallel plate geometry with a diameter of 50 mm, and the zero-gap size chosen was 1.00 mm. At the end of each experiment, the values of viscosity at different temperatures, for each DES were obtained.

#### 3.2.2.3 Density

The density of each DES was measured using an Anton Paar automatic kinematic viscometer model SVM 3001 in the temperature range of 20-50ºC with increments of 10ºC between measurements. Before starting the set of experiments, the densimeter was calibrated with water. For each measurement, approximately 4 mL of each DES was carefully taken out with a syringe of the vials containing DES, conditioned and injected slowly into the densimeter to prevent the formation of air bubbles inside the measuring device, which would affect the quality of each test and density value measured. The densimeter was cleaned with distilled water and dried before measuring new samples. The uncertainty of the densimeter was ±0.0001 $g.cm^{-3}$. In some cases, in particularly ChCl:MA (with and without CA), LA:L-Pro:W (with and without CA) conditioned at $a_w$=0.112 and ChCl:MA conditioned at $a_w$=0.529, density measurements could not be carried out in the densimeter, due to the high viscosity of the DES, and in these cases density was determined by the gravimetric method. In this method, 1 mL of DES was taken out with a syringe from the desiccator that was in the controlled temperature room at 30ºC and weighed in an analytical balance, and the corresponding mass was observed. Three independent measurements were done, and the mean value is presented. The uncertainty of the analytical balance was ±0.0001 g.

### 3.2.3 $CO_2$ Henry's Constant and $CO_2$ diffusion coefficient determination

$CO_2$ Henry's constant and diffusion coefficient of $CO_2$ measurements were carried out for each prepared DES to determine the Henry's constant and diffusion coefficient of $CO_2$.

Figure 3.2 depicts the experimental setup that was used to determine $CO_2$ Henry constant and diffusivity. To perform these measurements, both the absorption (AC) and the gas (GC) compartments were placed in a water bath that was kept at a constant temperature of 30 °C by means of a temperature controller (TC). Initially, GC compartment was purged with $CO_2$. For each experiment, 0.5 g of DES were placed into the AC inside a small, open glass flask. Next, the GC was pressurized with $CO_2$, keeping valve 1 opened while valve 2 was closed, until a constant value of relative pressure was attained (0.7 bar). Valve 1 was closed, and the system was left to stabilize for at least 1 hour. The $CO_2$ expansion into the absorption chamber (AC) would start, by opening valve 2. The pressure decay in the GC was monitored over time, which translates to the gas absorption by the DES thin film. After the pressure decay stage, once pressure value remains constant the test experiment was stopped.

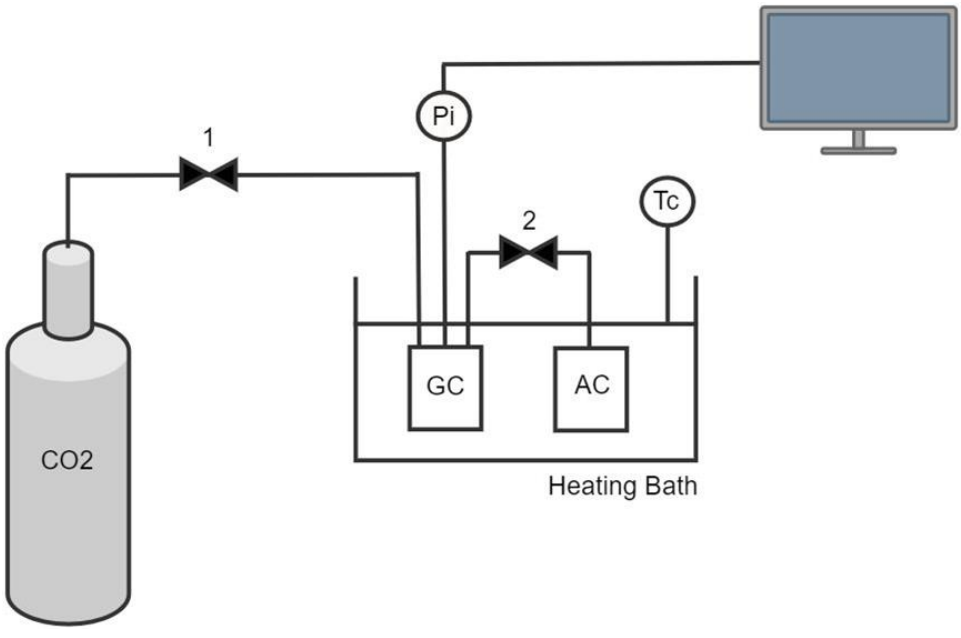


Figure 3.2- Experimental setup for $CO_2$ Henry's constant and diffusivity measurements.

The determination of $CO_2$ Henry constant and diffusion were then obtained mathematically, as previously reported[5], [38]. By merging Fick's 2nd law of diffusion for thin films with a mass

balance on the gas phase above the liquid, the pressure decay data, the $CO_2$ Henry's constant, and diffusion coefficient were obtained according to (Equation 3.1 and(Equation 3.2 :

$$\ln\frac{P}{P_0} = \frac{k}{H_{gas}}\sum_{n=0}^{\infty}\frac{1}{(2n+1)^2}\left\{exp\left[-\frac{(2n+1)^2\pi^2 D_{gas}t}{4L^2}\right]-1\right\} \text{(Equation 3.1)}$$

$$\text{with} \qquad k = \frac{8RTV_{solvent}\rho_{solvent}}{\pi^2 V_{gas} MW_{solvent}} \text{ (Equation 3.2)}$$

where $P$ and $P_0$ are the value of pressure over time and pressure after opening the valve that connects the AC to the GC (mbar); $H_{gas}$ is Henry's constant; $D_{gas}$ is the gas diffusion coefficient in the solvent ($cm^2.s^{-1}$); $L$ is the solvent film height (cm); $V_{solvent}$ ($cm^3$) and $V_{gas}$ ($cm^3$) are the volumes of solvent in the AC and $CO_2$ in the GC, respectively; $\rho_{solvent}$($g.cm^{-3}$) and $MW_{solvent}$(g/mol) are the density and molecular weight of the solvent, respectively.
Subsequently, Henry's constant ($H_{gas}$) and the diffusion coefficient ($D_{gas}$) were obtained for the different DES, by adjusting (Equation 3.1) to the obtained data of pressure decay over time in a MATLAB diffusion model program, using a non-linear regression method, by applying the Levenberg-Marquardt algorithm.

### 3.2.4 Supported Liquid Membrane (SLM) Preparation

The process used to immobilize the DES inside the membrane pores has been previously reported [5], [38]. Briefly, the PTFE hydrophilic polymeric membrane was placed in a desiccator and vacuum was applied for one hour to remove air inside the pores of the membrane support. Following this, the DES was injected using a syringe to completely fill all the membrane pores and the membrane was left in the desiccator for 1 hour. After that, excess DES was cleaned from the membrane surface with a thin paper. Before and after DES immobilization, membrane weight and thickness were measured using an analytical balance and a micrometer Metric (Aldrich). The membrane used had an area of 9.75 $cm^2$ and a thickness of 56.2 μm.

### 3.2.5 Supported DES Liquid Membrane permeability and ideal selectivity

Gas permeation tests for $CO_2/CH_4$ mixtures with different compositions were carried out. The purpose of these tests was to determine the permeability and selectivity of DES supported membrane. The apparatus consists of a stainless-steel cell with two identical compartments divided by the membrane under test, which was kept inside an oven (Paralab) with a controlled temperature of 30°C. Two mass flow controllers, MFC1 and MFC2 (Paralab), connected to the gas bottles of $CO_2$ and $CH_4$ —which were mixed inside the gas mixture box before going into the membrane module's feed compartment—controlled the flow rate of each gas. The total feed flow rate used was 200 mL/min for all experiments, and gas stream compositions for each test were controlled using mass-flow controllers. A back pressure regulator (BPR) was utilized to regulate the experimental pressure to 1 bar. During the experiment, helium (He) was employed as a sweep gas on the permeate compartment (MFC3) with a flow rate of 5 mL/min. The flow rate of the permeate stream was measured by a mass flow meter (MFM). An Agilent gas chromatograph (GC) 7890B, which employed Helium (He) as the gas carrier and was equipped with a thermal conductivity detector, was used to analyze the compositions of the feed and permeate. As previously mentioned, the tests were conducted at various gas compositions, as shown in Table 3.5, to replicate conditions similar to those of biogas streams. Three replica of each mixed gas composition were tested for both feed and permeate [5], [41].

Table 3.5- Molar fraction of the gas compositions of $CO_2$ and $CH_4$ used during permeation tests.

| **$CO_2$ (%)** | **$CH_4$ (%)** |
|---|---|
| 0 | 100 |
| 20 | 80 |
| 40 | 60 |
| 60 | 40 |
| 100 | 0 |

Results obtained from the permeability tests were used to determine the permeability results for pure gases through the PFTE supported liquid membrane. To obtain the permeability for $CO_2$ and $CH_4$, (Equation 3.3) was used:

$$Permeability_{gas} = \frac{Q \times l}{A \times p} \text{(Equation 3.3)}$$

in which $Q$ ($cm^3.s^{-1}$) represents the partial gas flowrate of $CO_2$ or $CH_4$ in the permeate and $l$ (cm), $Permeability_{gas}$ represents the membrane permeability (Barrer), $A$ represents the area of membrane used and pressure (p) is the pressure used during the permeation tests.

After obtaining the results for $CO_2$ and $CH_4$ permeability the ideal selectivity ($\alpha_{CO_2/CH_4}$) was calculated by dividing the permeabilities of both pure gases (Equation 3.4):

$$\alpha_{CO_2/CH_4} = \frac{P_{CO_2}}{P_{CH_4}} \text{ (Equation 3.4)}$$

# 4 Results and Discussion

## 4.1 Characterization of Deep Eutectic Systems

The prepared DES were characterized to later relate their physicochemical properties, with their ability for gas absorption and/or separation.

#### 4.1.1.1 FTIR-ATR

The Fourier Transform infrared spectroscopy (FTIR) technique allowed for the chemical characterization of the selected DES, making it able to verify the vibrations of the compound's characteristic chemical bonds in the DES while also being used to confirm the formation of each DES. All DES were analyzed by FTIR before the start of the conditioning process.

##### 4.1.1.1.1 ChCl:MA

The FTIR-ATR spectra of DES ChCl:MA (1:1) is shown in Figure 4.1, as well as the FTIR spectra for its individual components, choline chloride and malonic acid. As can be seen by analyzing the three spectra, the DES spectrum a combination of the spectra of its pure components with the exception of a frequency shift from 1695 $cm^{-1}$ to 1717 $cm^{-1}$. A broad strong peak at 1965 $cm^{-1}$ in the malonic acid spectrum represents the stretching of the carbonyl group (C=O) of this acid and represents two dimer rings (related to two identical C=O groups of malonic acid) with identical hydrogen bonding strength that are mostly free in the DES mixture, while the OH groups are bonded to the $Cl^-$ of ChCl[47]. In the DES, this peak becomes more intense and shifts to a higher wavenumber (1717 $cm^{-1}$). On the other hand, the broad band at 3700-3200 $cm^{-1}$ of hydroxyl (-OH) stretching region represents the formation of various hydrogen bonds such as the strong bond formed between hydroxyl groups of MA and the Chloride anion of ChCl (OH—$Cl^-$) and the hydrogen bonds formed between MA molecules (O---HO)[47]. The ChCl hydroxyl peak at 3222 $cm^{-1}$ disappeared in the DES spectra, representing a significant dissociation of the original OH-$Cl^-$ bonds in ChCl to form hydrogen bonds with the hydroxyl groups of MA. The bands associated to choline chloride, -$CH_3$, -$CH_2$, -CCO and -CH are also present in the FTIR spectra of the DES associated to wavenumbers 1482 $cm^{-1}$, 1083 $cm^{-1}$, 952 $cm^{-1}$, and 531 $cm^{-1}$ respectively, meaning that the structure of $Ch^+$ ion is still present in the DES structure.

On the other hand, the bands associated with -$CH_2$ and -CCO and -CH can also be observed in the spectrum of malonic acid at the same wavenumbers, as well as a band associated with a C-O bond at 1216 $cm^{-1}$, meaning that the structure of the carboxylic acid is also still present in the DES structure. When comparing the FTIR results of pure ChCl:MA with ChCl:MA_CA, it is possible to observe some noticeable changes related to the presence of the enzyme, due to interactions between DES components and CA. Firstly in the FTIR graph of the DES with enzyme the broad band at 3700-3200 $cm^{-1}$ of hydroxyl (-OH) stretching region became more intense, and the strong peak at 1717 $cm^{-1}$ representative of the carbonyl group of MA lost intensity and now is represented by 2 peaks. This last difference noticed when comparing the FTIR graph of the DES with enzyme without enzyme happens probably because an amide band of CA is also typically represented in that wavelength interval of 1600-1700 $cm^{-1}$ (mainly due to C=O stretching) which is the most sensitive spectral region of protein components and represents the presence of the enzyme in the DES [48].

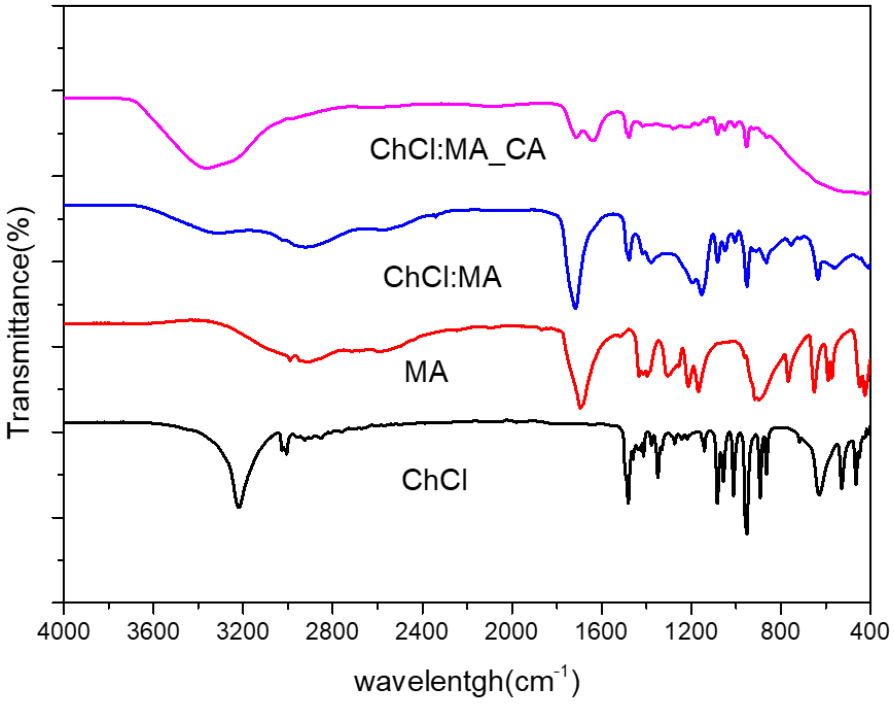


Figure 4.1-FTIR spectra for pure components and for DES ChCl:MA and ChCl:MA_CA.

#### 4.1.1.1.2 ChCl:LA

The FTIR spectra of the DES ChCl:LA (1:2) is shown in Figure 4.2, alongside the FTIR spectra for the individual components, Choline Chloride and Lactic Acid. As for the previous case, the FTIR spectra obtained for the DES is a combination of the spectra of its individual components but in this case with 2 frequency shifts. The band ranging from 3700 to 3200 $cm^{-1}$ in the DES spectrum, associated with the -OH groups stretching broadened and intensified, providing evidence of formation of the hydrogen bonds formed between the -OH groups present in the alcohol functional group of Lactic Acid and the nitrogen ion in choline chloride, and indicating the successful DES formation[49]. The ChCl hydroxyl peak at 3222 $cm^{-1}$ is not observed in the DES spectrum, representing a dissociation of the OH-$Cl^-$ bonds of ChCl. The formation of broader peaks in ChCl:LA indicates the formation of hydrogen bonds between the nitrogen in the amine group and the hydrogen from the carboxyl group in lactic acid. The peak at 1717 $cm^{-1}$ in the lactic acid spectrum represents the C=O stretching of the carboxylic groups. In the DES spectrum this sharp peak shift to a higher wavenumber (1723 $cm^{-1}$), which can be taken as evidence for hydrogen bond formation associated with O=C-O-H…$N^+$ (lactic acid-Choline Chloride)[49]. On the other hand, the peak at 1206 $cm^{-1}$ in the DES spectrum represents the stretching of C-O group present in Lactic Acid. This peak shifts from 1213 $cm^{-1}$ in lactic acid spectrum, to 1206 $cm^{-1}$ in the DES spectrum, representing that stretching of this bond occurred during DES formation. Furthermore, the vibrations from 1450 to 800 $cm^{-1}$ represent C-O stretching, O-H bending and C—H stretching from the hydroxyl and alkane groups in the acid's structure.

When comparing the FTIR results of ChCl:LA with ChCl:LA_CA, it is possible once again to observe some noticeable changes related to the presence of the enzyme, due to interactions between DES components and CA. In the FTIR graph of the DES with enzyme the broad band at 3700-3200 $cm^{-1}$ of hydroxyl (-OH) stretching region became more intense, and the strong peak at 1723 $cm^{-1}$ representative of the carbonyl group of LA lost intensity and now is represented by 2 peaks, such as in ChCl:MA. Similarly to the other choline chloride-based DES this happened probably because an amide band of CA is usually represented in that wavelength interval of 1600-1700 $cm^{-1}$ (mainly due to C=O stretching) which is the most sensitive spectral region of protein components and represents the presence of the enzyme in the DES [48].

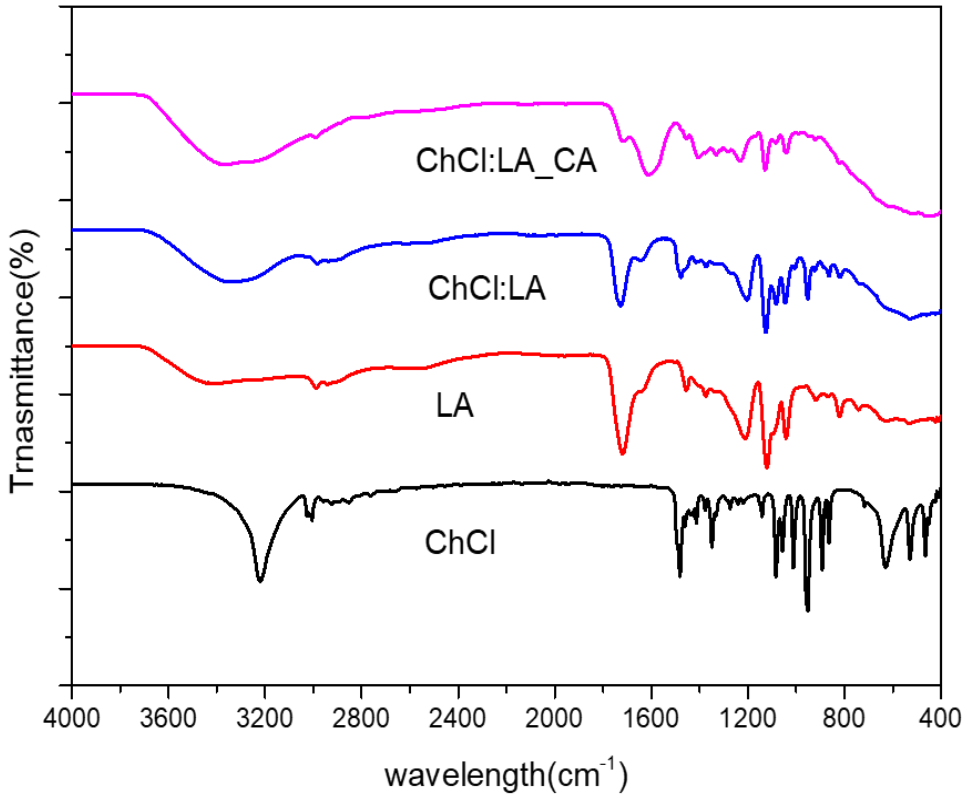


Figure 4.2-FTIR spectra for pure components and for DES ChCl:LA and ChCl:LA_CA.

#### 4.1.1.1.3 Gly:L-Pro

For the DES Gly:L-Pro (2.5:1) and its components, FTIR spectra is shown in Figure 4.3 and the DES spectrum is again a combination of the spectra of its pure components except of a frequency shift. For glycerol, the characteristic peaks of C-OH stretching, C-H stretching and C-O stretching and $CH_2$ group are represented at 3292 $cm^{-1}$, 2932 $cm^{-1}$, 2879 $cm^{-1}$, 1110 and 1030 $cm^{-1}$ and 850$cm^{-1}$ respectively. On the other hand, for pure L-Proline, the characteristic peaks of N-H stretching, C-H stretching ,C-H bending, C=O stretching, N-H bending, C-N stretching, C-O stretching, $CH_2$ group, C((C=O)O) bond are identified, and located at 3295 $cm^{-1}$, 2932 and 2879 $cm^{-1}$, 1614 $cm^{-1}$, 1556 $cm^{-1}$, 1375 $cm^{-1}$, 1169$cm^{-1}$, 1030$cm^{-1}$ , 850 and 450 $cm^{-1}$ respectively[50]. Moreover, the ring belonging to L-Proline is also represented by the peak at 1086 $cm^{-1}$. Each one of these peaks from the 2 pure components is also represented in the FTIR spectra of the DES, at the same wavenumber, confirming their presence in DES structure. Moreover, as can be seen in the FTIR spectrum of the DES, the peak that represents the stretching vibration of the C-OH bonds of glycerol shifts from 3292 $cm^{-1}$ to 3272 $cm^{-1}$, which can indicate the formation of hydrogen bonds between L-Proline and Glycerol and consequently DES formation[50].

When comparing the FTIR results of pure Gly:L-Pro with Gly:L-Pro_CA, it is also possible to observe some noticeable changes related to the presence of the enzyme, due to interactions between DES components and CA. Once again, there is a difference in the broad band at 3700-3200 $cm^{-1}$ of hydroxyl (-OH) region, that became more intense when compared to the DES without enzyme and as in with the other DESs there was also a shift and decrease of intensity in the peak representative of the carbonyl group of L-Proline at 1614 $cm^{-1}$. Similarly to other DES, this is observed probably because an amide band of CA is usually represented in that wavelength interval of 1600-1700 $cm^{-1}$ (mainly due to C=O stretching) which is the most sensitive spectral region of protein components and represents the presence of the enzyme in the DES [48].

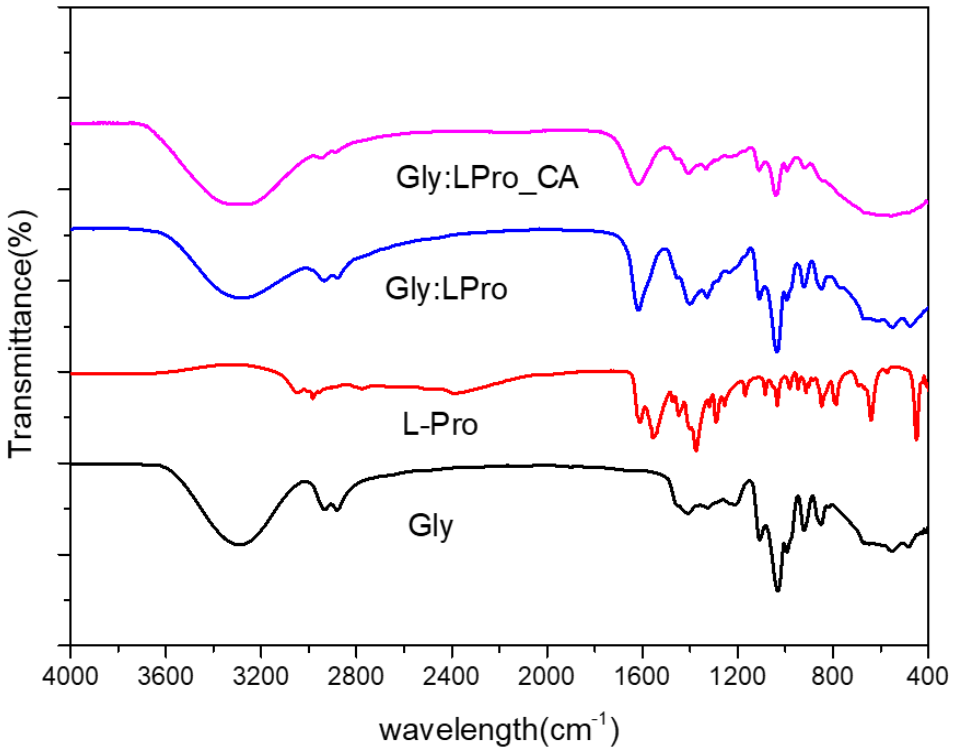


Figure 4.3-FTIR spectra for pure components and for DES Gly:L-Pro and Gly:L-Pro_CA.

#### 4.1.1.1.4 LA:L-Pro:W

For DES Lactic Acid:L-Proline:Water (1:1:1) and its pure components, FTIR spectra are represented in Figure 4.4. As can be seen by comparing the two spectra (Lactic acid and L-Proline), the DES spectrum is also a combination of the spectra of its pure components except of a frequency shift. In lactic acid, the -OH band is very wide because it contains two different types

of OH groups, the one present in the acid functional group (-COOH) and the other one present in the alcohol functional group(-OH). The -OH group in the acid group absorbs between 2500 and 3200 $cm^{-1}$, and the one present in the alcohol one between 3700 and 3230 $cm^{-1}$, which makes this band very wide covering the whole range from 2500 to 3700 $cm^{-1}$[49]. In that same region it is also represented the C-H bonds of the molecule at 2986 $cm^{-1}$ and 2940 $cm^{-1}$. In the DES spectra, the band ranging from 3700-3200 $cm^{-1}$ representing OH stretching bonds broadens representing establishment of hydrogen bonds between L-Proline and Lactic Acid, or in other words DES formation. The peak at 2945 $cm^{-1}$ represents the C-H bonds present in both LA and L-Pro[51]. The peak at 1717 $cm^{-1}$ in the Lactic Acid spectra represents the C=O stretching of the carboxylic group[52]. The peak which represents the N-H bond bending present in L-proline shifts from 1584$cm^{-1}$ to 1619 $cm^{-1}$ in the DES spectra and gets broader, which is an indication of hydrogen bond formation between the pure components. Furthermore, the peak at 1367$cm^{-1}$ in the DES spectra represents C-H bending and it can be also seen in both pure components spectra. The peaks at 1222 $cm^{-1}$ and 1126 $cm^{-1}$ in the DES spectra represent C-O stretching and C-N stretching[51]. When comparing the FTIR results of pure LA:L-Pro:W with LA:L-Pro:W_CA, it is also possible to observe some noticeable changes related to the presence of the enzyme, due to interactions between DES components and CA. As in the other DESs, there is a big difference in the broad band at 3600-3200 $cm^{-1}$ of hydroxyl (-OH) region, that became a lot more intense when compared to the DES without enzyme. It is also noticeable a slight decrease in intensity in the peak corresponding to C-H bonds at 2986 $cm^{-1}$ and there is a decrease of intensity in the peak representative of the C=O stretching of the carboxylic group of Lactic acid at 1717 $cm^{-1}$. As previously mentioned, this is observed probably because an amide band of CA is usually represented in that wavelength interval of 1600-1700 $cm^{-1}$ (mainly due to C=O stretching) which is the most sensitive spectral region of protein components and represents the presence of the enzyme in the DES [48].

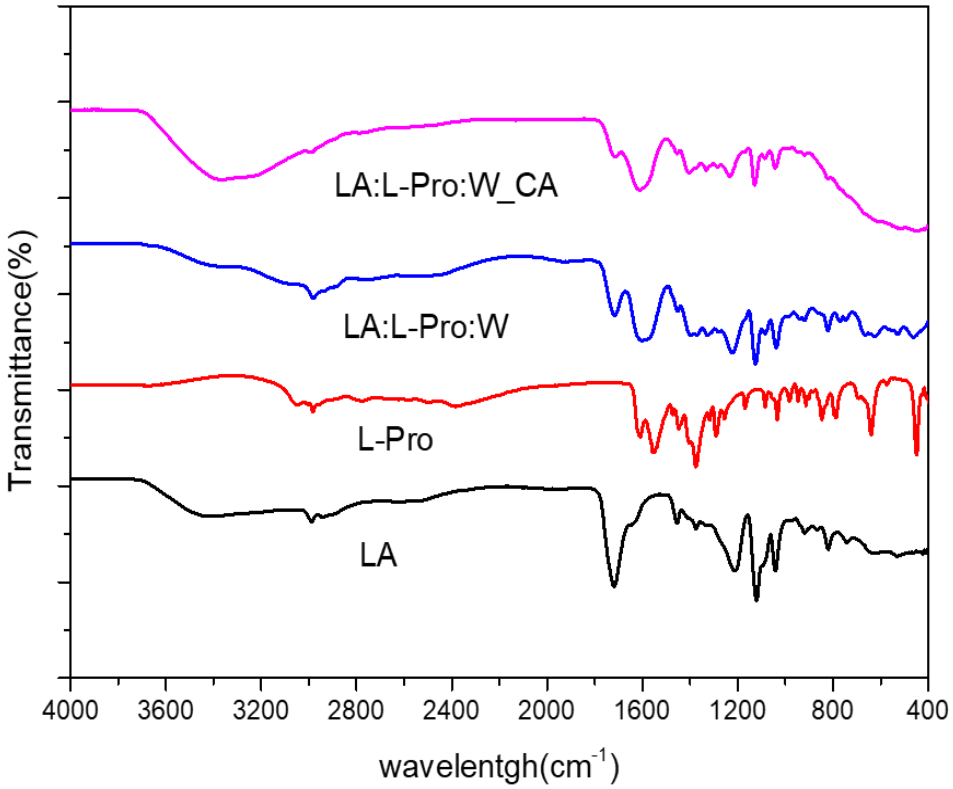


Figure 4.4-FTIR spectra for pure components and for DES LA:L-Pro:W and LA:L-Pro:W_CA.

#### 4.1.1.2 Viscosity

Viscosity is a crucial property of DES because it affects their suitability for certain applications as solvents, and in the case of this work for gas mass transfer. Viscosity is dependent on the size of the DES components, since it is related to the free volume of the DES, hydrogen bonding, electrostatic interactions, and Van der Waals interactions established between the DES components. As a result, the components' chemical character, its molar ratio, temperature, and water content all affect the viscosity value[9]. Figures 4.5 to Figures 4.11 show the viscosity results of the studied DES from 20 to 80ºC, at the 4 different water activity levels.

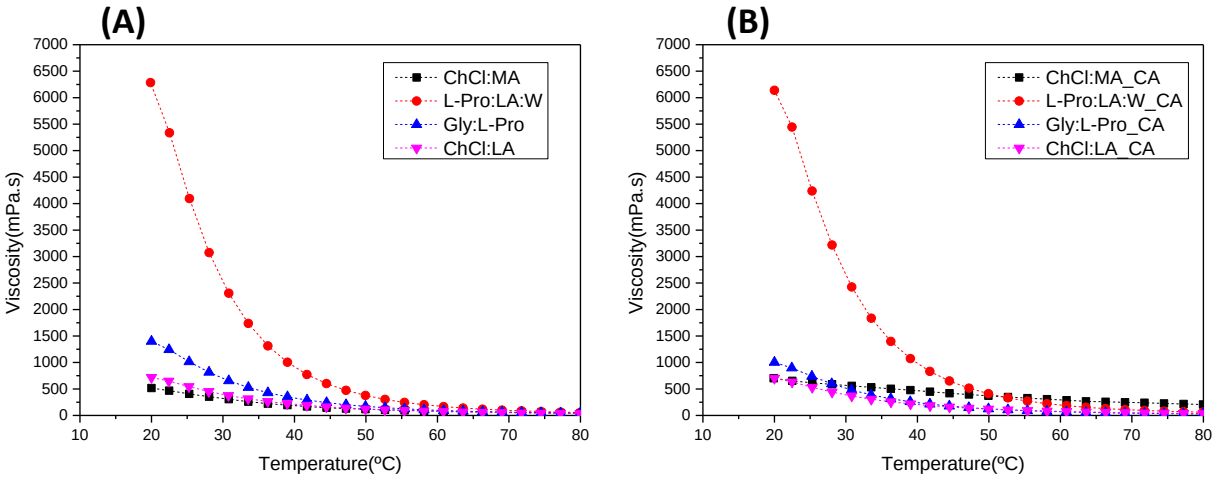


Figure 4.5-Effect of temperature in DES viscosity at $a_w$=0.112: (A)without enzyme, (B)with enzyme.

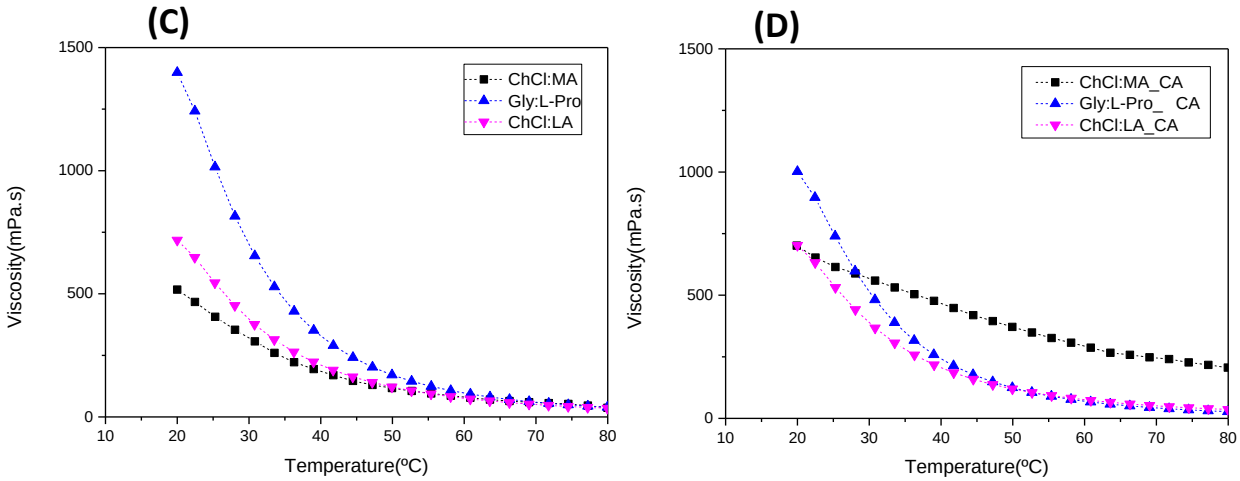


Figure 4.6-Effect of temperature in ChCl:MA, Gly:L-Pro and ChCl:LA viscosity at $a_w$=0.112: (C)without enzyme, (D)with enzyme.

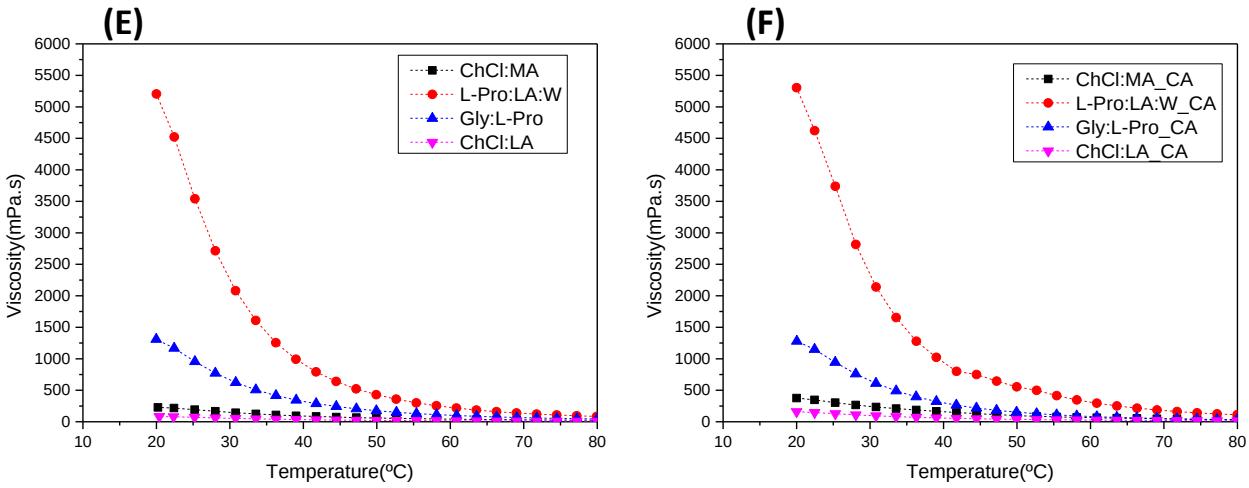


Figure 4.7-Effect of temperature in DES viscosity at $a_w$=0.226: (E)without enzyme, (F)with enzyme.

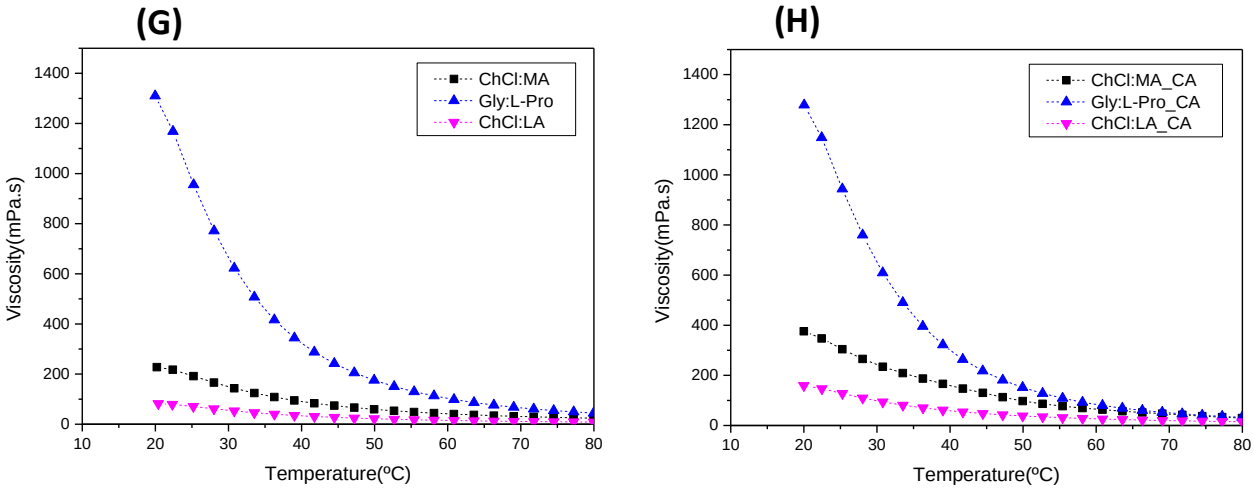


Figure 4.8- Effect of temperature in ChCl:MA, Gly:L-Pro and ChCl:LA viscosity at $a_w$ =0.226: (G)without enzyme, (H)with enzyme.

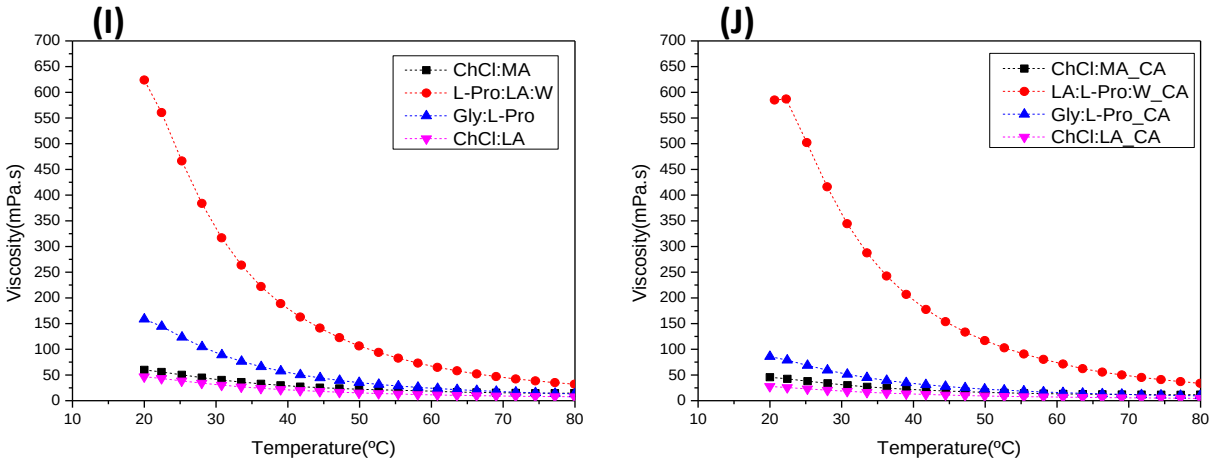


Figure 4.9 -Effect of temperature in DES viscosity at different $a_w$ =0.529: (I)without enzyme, (J)with enzyme.

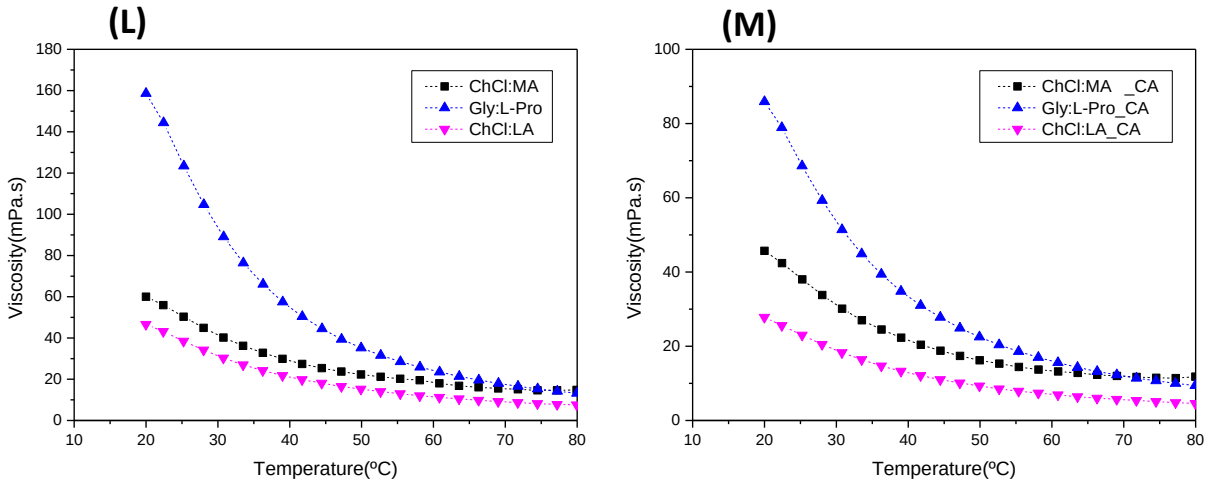


Figure 4.10-Effect of temperature in ChCl:MA, Gly:L-Pro and ChCl:LA viscosity at $a_w$ =0.529: (L)without enzyme, (M)with enzyme.

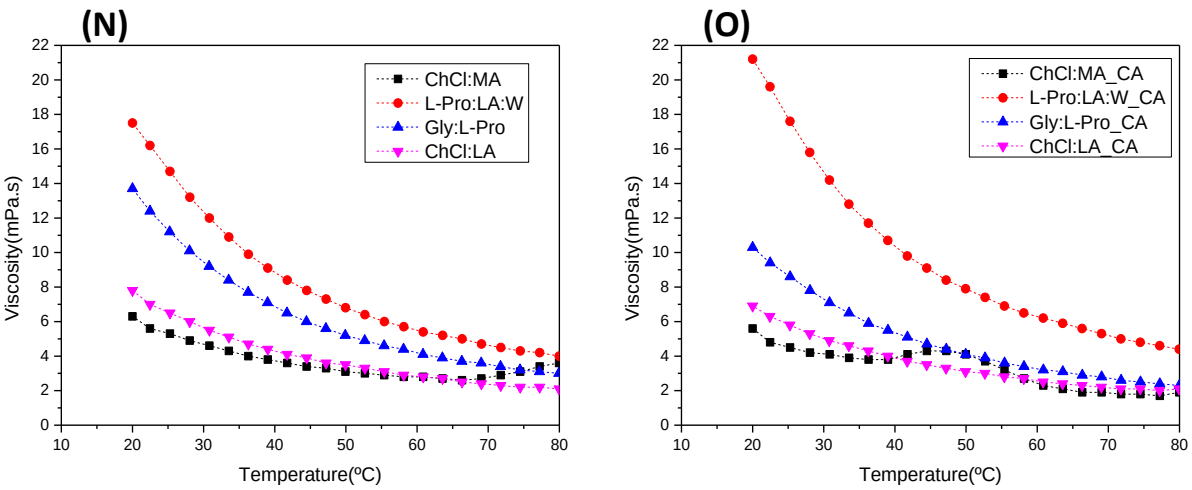


Figure 4.11-Effect of temperature in DES viscosity at different $a_w$ =0.843: (N)without enzyme, (O)with enzyme.

As can be observed in all DES tested, viscosity decreases with the increase in temperature. The LA:L-Pro:W DESs shows the highest viscosity at 30°C but these values decrease significantly with the increase in temperature. For example, the viscosity changes for LA:L-Pro:W DES from 20 to 80°C decrease from 6 284.5 mPa.s to 54.3 mPa.s (for $a_w$=0.112), 5 204.2 mPa.s to 84.4 mPa.s (for $a_w$=0.226), 623.9 to 32.1 mPa.s (for $a_w$=0.529) and 17.5 to 4 mPa.s (for $a_w$=0.843). The dependance of DES viscosity on temperature and strength of the intermolecular forces in each DES can be quantified by the Activation Energy ($E_a$) of each DES [46] which can be obtained by applying the linearization of the Arrhenius model (Equation 4.1) and $\mu_0$ is the pre-exponential factor for the liquid system [53]:

$$ln\mu = ln\mu_0 + \frac{E_a}{RT} \text{ (Equation 4.1)}$$

As can be seen in Table 4.1 and Table 4.2 generally higher viscosities such as the ones obtained for LA:L-Pro:W and Gly:L-Pro have higher $E_a$ values, which is expected since higher viscosity means stronger interactions between DES components, while lower viscosity DES such as ChCl:LA and ChCl:MA show lower $E_a$values, which is also expected since lower viscosity means weaker interactions between DES components. Moreover, the obtained results help confirm that DES viscosity is significantly influenced by HBA-HBD intermolecular interactions [46]. According to this fact, it can also be concluded that LA:L-Pro:W and Gly:L-Pro are the DES where a change in temperature has a higher impact in viscosity, while on the other

hand on the choline chloride based DES its influence on this property is generally less pronounced, as can be confirmed by Table 4.1.

Table 4.1- Activation Energy calculated using Arrhenius equation for the prepared DES.

| DES | $a_w$ | Water Content (wt%) | μ (mPa.s) (30ºC) | $E_a$(kJ/mol) | $R^2$ |
|---|---|---|---|---|---|
| ChCl:MA | 0.112 | 4.778 | 306.9 | 62.01 | 0.86 |
| | 0.226 | 5.967 | 143.4 | 36.81 | 0.99 |
| | 0.529 | 12.012 | 40.2 | 20.71 | 0.95 |
| | 0.843 | 39.976 | 4.6 | 10.06 | 0.71 |
| LPro:LA:W | 0.112 | 1.932 | 2307.3 | 58.80 | 0.96 |
| | 0.226 | 3.003 | 2080.6 | 60.73 | 0.99 |
| | 0.529 | 9.145 | 316.9 | 43.27 | 0.99 |
| | 0.843 | 37.452 | 12 | 21.27 | 0.99 |
| Gly:L-Pro | 0.112 | 1.048 | 654.4 | 47.29 | 0.99 |
| | 0.226 | 4.865 | 622.7 | 49.80 | 0.99 |
| | 0.529 | 11.282 | 89.1 | 36.25 | 0.99 |
| | 0.843 | 39.777 | 9.2 | 21.79 | 0.99 |
| ChCl:LA | 0.112 | 1.821 | 375.9 | 29.13 | 0.95 |
| | 0.226 | 6.183 | 53.1 | 34.02 | 0.99 |
| | 0.529 | 13.847 | 30.3 | 26.79 | 0.99 |
| | 0.843 | 42.126 | 5.5 | 18.69 | 0.99 |

Table 4.2- Activation Energy calculated using the Arrhenius equation for the DES prepared with CA.

| DES | $a_w$ | Water Content (wt%) | μ (mPa.s) (30°C) | Ea(kJ.mol$^{-1}$) | $R^2$ |
|---|---|---|---|---|---|
| ChCl:MA_CA | 0.112 | 1.882 | 559.1 | 61.68 | 0.88 |
| | 0.226 | 5.897 | 234.3 | 36.81 | 0.99 |
| | 0.529 | 12.231 | 30.1 | 20.71 | 0.95 |
| | 0.843 | 40.036 | 4.1 | 16.64 | 0.85 |
| L-Pro:LA:W_CA | 0.112 | 2.098 | 2426.2 | 60.37 | 0.95 |
| | 0.226 | 2.926 | 2140.2 | 42.93 | 0.99 |
| | 0.529 | 9.066 | 344.3 | 43.09 | 0.99 |
| | 0.843 | 37.152 | 14.2 | 22.60 | 0.99 |
| Gly:L-Pro_CA | 0.112 | 1.619 | 620.5 | 45.52 | 0.99 |
| | 0.226 | 4.472 | 609.4 | 54.54 | 0.99 |
| | 0.529 | 11.456 | 51.4 | 32.36 | 0.99 |
| | 0.843 | 39.542 | 7.1 | 21.51 | 0.99 |
| ChCl:LA_CA | 0.112 | 2.504 | 366.9 | 34.29 | 0.95 |
| | 0.226 | 6.238 | 94.1 | 34.91 | 0.99 |
| | 0.529 | 14.001 | 18.3 | 25.69 | 0.99 |
| | 0.843 | 42.268 | 4.9 | 17.93 | 0.99 |

When it comes to the effect of the presence of CA in viscosity values as function of temperature, it can be observed in more detail in Figure 4.7 and Table 4.2. As it can also be seen in previous Figures 4.5 to Figure 4.11, that the values obtained that viscosity values generally follow the same order for DES with and without CA for all $a_w$: LA:L-Pro:W> Gly:L-Pro>ChCl:MA≈ChCl:LA.

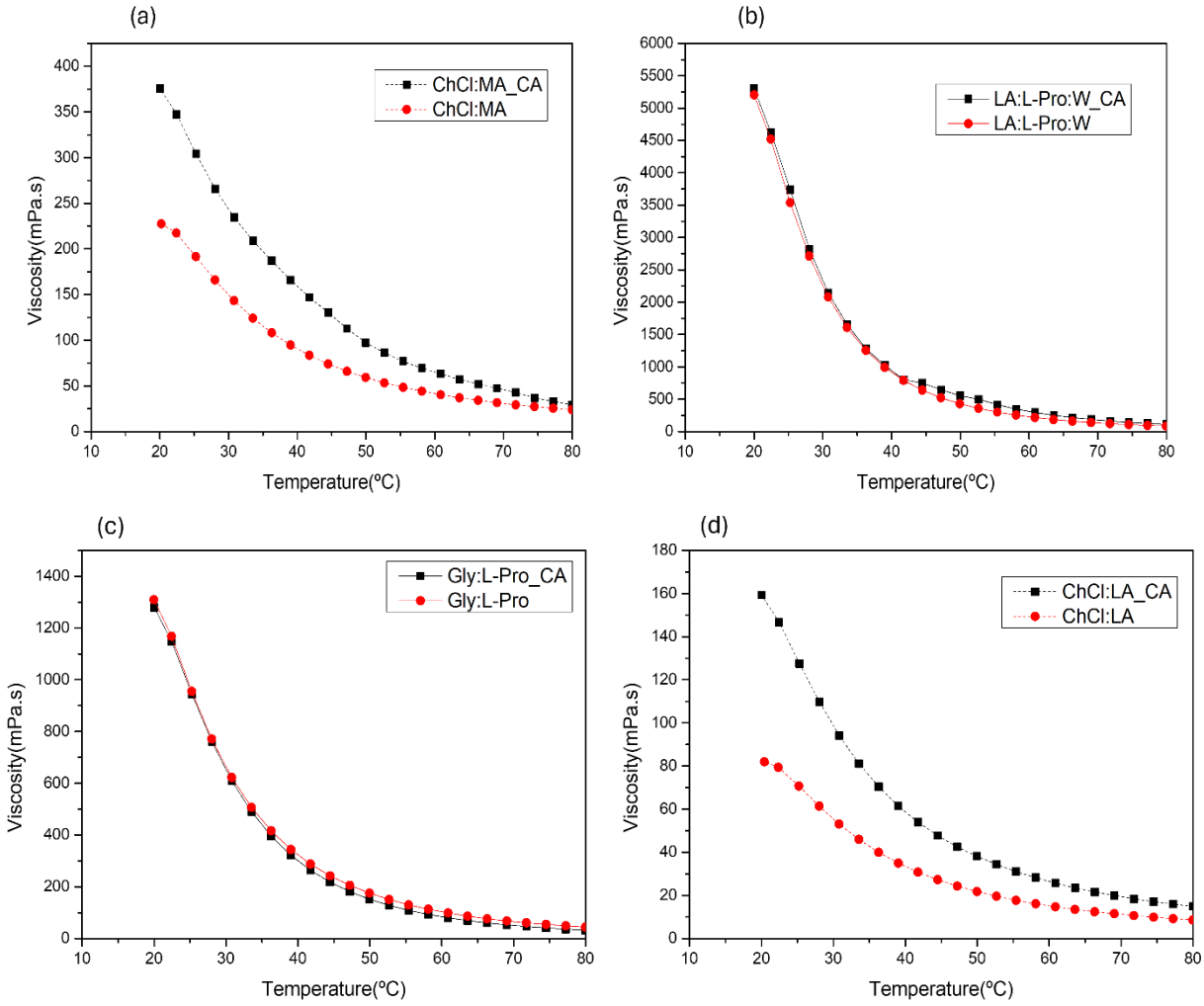


Figure 4.7- Effect of CA in viscosity values as a function of temperature in DES pre-equilibrated in $a_w$=0.226.

In order to understand the impact of water activity on viscosity (at 30ºC) of the different DES prepared in this work, with and without the presence of carbonic anhydrase (CA), viscosity measurements were performed and are presented in Figure 4.10.

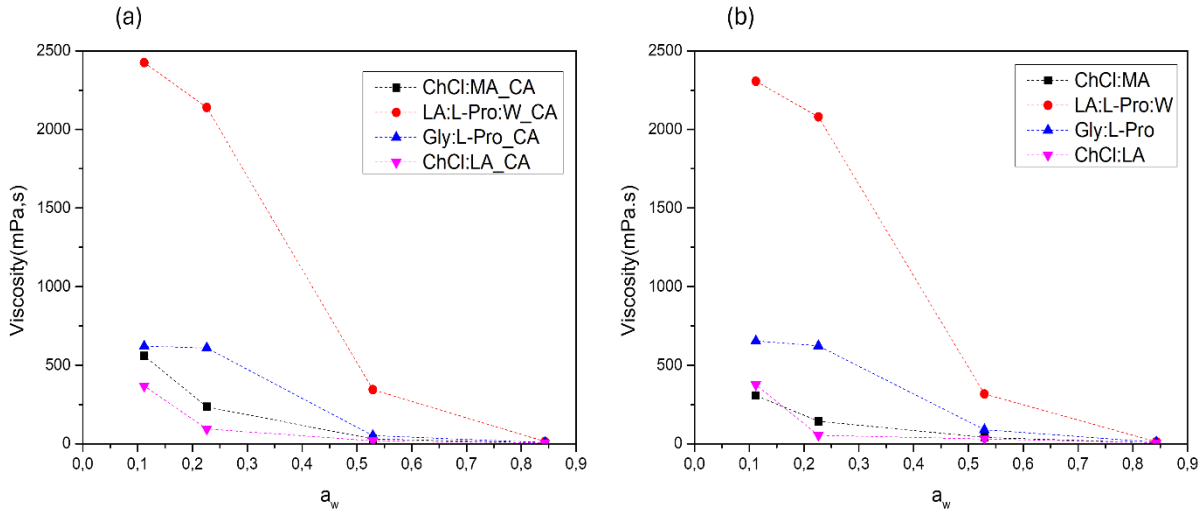


Figure 4.8-Water equilibrated DES viscosity with and without CA as function of water activity, at 30°C.

As previously mentioned, the water content has a major effect in DES viscosity. The presence of water molecules can disrupt/weaken the intramolecular forces between DES components leading to a decrease of resistance to flow/lower viscosity. This trend can be confirmed in Table 4.3 and Table 4.4, and also in as generally the viscosity of each DES decreases as their water content increases not only in the same $a_w$ level but also when comparing different $a_w$.

From the results presented in Figure 4.10, LA:L-Pro:W exhibits the highest viscosity across all water activity levels at 30°C but these values decrease drastically with increase of water activity compared to the other DES, particularly when comparing $a_w$=0.226 and $a_w$=0.529.

From the results above, it is also observed that for Choline Chloride based DES, the one with malonic acid as the hydrogen bond donor (HBD) is generally more viscous, for the different water activities tested. Florindo *et al.*[54] have investigated the viscosity of ChCl:carboxylic acid DES(oxalic acid, glycolic acid, malonic acid, glutaric acid, and levulinic acid) and concluded that DES containing a diacid are more viscous than the ones containing a monoacid. This relationship is confirmed according to the results obtained since, besides water content difference, one of the main differences between malonic acid and lactic acid is the number of carboxylic groups, as the former has 2 carboxylic groups and the latter only 1 carboxylic group, leading probably to the formation of more hydrogen bonds between choline chloride and malonic acid, leading to a higher viscosity[54]. On the other hand, bigger HBD molecules result in a higher viscosity of the DES as it can affect the mobility of the system. This can be attributed to the fact that larger molecules have lower overall mobility[55]. Between malonic acid ($M_w$=104.06 g/mol) and lactic acid ($M_w$=90.08 g/mol), malonic acid is a bigger molecule which

can be also another explanation for why the DES choline chloride:malonic acid is generally more viscous than choline chloride:lactic acid at the same $a_w$. Additionally, the highest viscosity values for ChCl:MA can be also credited to the formation of dimer chains between malonic acid molecules, which can further restrict the mobility of this DES molecules[55]. When in comparison with values found in literature for the studied DES, the viscosity values obtained for ChCl:MA across all water level activities are lower in comparison to 982.9 mPa.s obtained by Florindo *et al*.[54] at 30ºC, which reflects the impact of conditioning in this property.

Regarding the effect of the presence of CA in viscosity values at 30ºC, it can be noticed from Figure 4.10, that DES with and without CA exhibit identical behaviors across different $a_w$ level. On the other hand it can also be seen in Table 4.3 and Table 4.4, that generally the values obtained that viscosity generally follows the same order for DES with and without CA for all $a_w$: LA:L-Pro:W>Gly:L-Pro>ChCl:MA>ChCl:LA.

Table 4.3- Water Content, viscosity and density of the pre-equilibrated DES in the different salts at 30ºC.

| DES | $a_w$ | Water Content (wt%) | μ(mPa.s) | ρ (g.cm$^{-3}$) |
|---|---|---|---|---|
| ChCl:MA | 0.112 | 4.778 | 306.9 | 1.241 |
| | 0.226 | 5.967 | 143.4 | 1.210 |
| | 0.529 | 12.012 | 40.2 | 1.204 |
| | 0.843 | 39.976 | 4.6 | 1.134 |
| LPro:LA:W | 0.112 | 1.932 | 2307.3 | 1.328 |
| | 0.226 | 3.003 | 2080.6 | 1.256 |
| | 0.529 | 9.145 | 316.9 | 1.240 |
| | 0.843 | 37.452 | 12 | 1.189 |
| Gly:L-Pro | 0.112 | 1.048 | 654.4 | 1.263 |
| | 0.226 | 4.865 | 622.7 | 1.252 |
| | 0.529 | 11.282 | 89.1 | 1.236 |
| | 0.843 | 39.777 | 9.2 | 1.168 |
| ChCl:LA | 0.112 | 1.821 | 375.9 | 1.173 |
| | 0.226 | 6.183 | 53.1 | 1.165 |
| | 0.529 | 13.847 | 30.3 | 1.163 |
| | 0.843 | 42.126 | 5.5 | 1.108 |

Table 4.4- Water Content, viscosity and density of the pre-equilibrated DES with enzyme in the different salts at 30ºC.

| DES | $a_w$ | Water Content (wt%) | μ(mPa.s) | ρ (g.cm$^{-3}$) |
|---|---|---|---|---|
| ChCl:MA _CA | 0.112 | 1.882 | 559.1 | 1.243 |
| | 0.226 | 5.897 | 234.3 | 1.212 |
| | 0.529 | 12.231 | 30.1 | 1.201 |
| | 0.843 | 40.036 | 4.1 | 1.125 |
| L-Pro:LA:W _CA | 0.112 | 2.098 | 2426.2 | 1.326 |
| | 0.226 | 2.926 | 2140.2 | 1.256 |
| | 0.529 | 9.066 | 344.3 | 1.243 |
| | 0.843 | 37.152 | 14.2 | 1.171 |
| Gly:L-Pro _CA | 0.112 | 1.619 | 620.5 | 1.258 |
| | 0.226 | 4.472 | 609.4 | 1.254 |
| | 0.529 | 11.456 | 51.4 | 1.237 |
| | 0.843 | 39.542 | 7.1 | 1.145 |
| ChCl:LA _CA | 0.112 | 2.504 | 366.9 | 1.168 |
| | 0.226 | 6.238 | 94.1 | 1.160 |
| | 0.529 | 14.001 | 18.3 | 1.157 |
| | 0.843 | 42.268 | 4.9 | 1.100 |

#### 4.1.1.3 Density

One of the most important characteristics of liquids is their density, which at specific pressure and temperature combinations, indicates their chemical structure compactness [56]. The density of DES can be higher or lower depending on how the molecules are organized in its structure or how the HBA and HBD species are packaged. Because DES are essentially constituted by holes/free space an increase in free space results in a drop in density[57]. According to literature, most DES densities are higher than density of water (between 1.0 and 1.35 g.cm$^{-3}$ at 25ºC)[57]. Hence, as it was done previously with viscosity, to understand the effect of water activity on density (at 30 ºC) of the DES used during this work, with and without the presence

of carbonic anhydrase (CA), the results obtained are presented in Figure 4.9, Table 4.3 and Table 4.4.

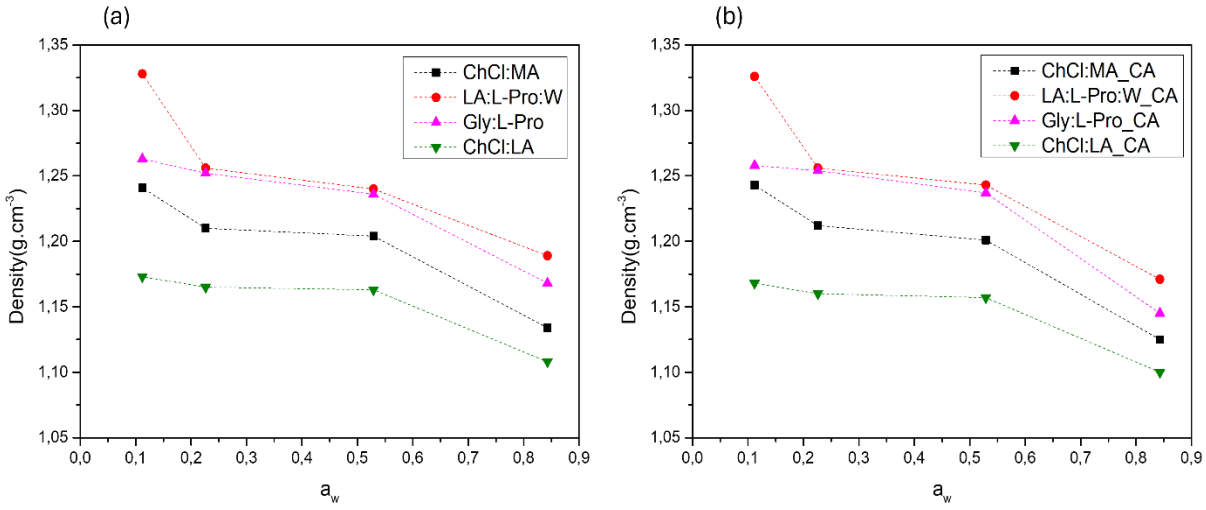


Figure 4.9- DES density with CA and without CA as function of water activity, at 30 °C.

L-Pro:LA:W presents higher density than Gly:L-Pro at a lower water activity ($a_w$=0.112), but at intermediate water activity levels ($a_w$=0.226 and $a_w$=0.529) its density decreases. This decrease can, like in viscosity, be explained by the influence of water in weakening interactions between DES components in the L-Pro:LA:W DES structure. In addition, there is an abrupt decrease in density for all the DES at $a_w$=0.843, which can again be explained by the change in organization of DES structure promoted by a higher water content.

Regarding the choline chloride-based DES, the effect of the HBD is also observed. When comparing ChCl:MA to ChCl:LA it is observed that ChCl:MA has higher density. This can be explained due to the higher density of its HBD (1.60 g.cm$^{-3}$) when compared to ChCl:LA (LA is the HBD with density of 1.209 g.cm$^{-3}$). On the other hand, similarly to the viscosity results, it is observed that the presence of an extra carboxylic group in MA leads to a higher density value for ChCl:MA across all $a_w$[58].

Bušic *et al*. [58] determined the density values of ChCl:MA and ChCl:LA at 30ºC, obtaining values of ρ=1.2112 g.cm$^{-3}$ for ChCl:MA and ρ=1.1380 g.cm$^{-3}$ for ChCl:LA. When in comparison to the results obtained in this work, it is possible to observe that for ChCl:MA similar values are obtained for $a_w$=0.226 (ρ=1.210 g.cm$^{-3}$) and $a_w$=0.529 (ρ=1.204 g.cm$^{-3}$) but for the remaining $a_w$ substantial differences were noticed: for $a_w$=0.112 it was obtained a higher value (ρ=1.241 g.cm$^{-3}$) and for $a_w$=0.843 where the value obtained was substantially lower (ρ=1.134 g.cm$^{-3}$)

which can be explained by the high water content value (39.98% wt$H_2O$/wtDES). On the other hand, some lesser differences are also observed in the results obtained for ChCl:LA : for $a_w$=0.112, $a_w$=0.226 and $a_w$=0.529 the density values ρ=1.173 g.cm$^{-3}$ , ρ=1.165 g.cm$^{-3}$ and ρ=1.163 g.cm$^{-3}$ respectively are higher in comparison to the one found in literature, and for $a_w$=0.843 the value obtained is lower(ρ=1.108 g.cm$^{-3}$ ).

Regarding the effect of the presence of CA in density values at 30ºC, it can be seen from Figure 4.9, that identically to viscosity that DES with and without CA display the same behaviors at varying $a_w$, and that the addition of CA does not have impact in DES density values. Moreover, as previously observed, density values for DES with and without CA generally follow the same order for all $a_w$: LA:L-Pro:W>Gly:L-Pro>ChCl:MA>ChCl:LA.

#### 4.1.1.4 $CO_2$ Diffusion Coefficients and Henry's Constant in DES

Table 4.5 shows the results obtained for the determination of the $CO_2$ diffusion coefficient ($D_{CO2}$) and Henry's constant (H) in the studied DES without CA pre-equilibrated in the lithium chloride salt ($a_w$ =0.112). For each case, two experiments were carried out, where the difference relied on the water content presented in Table 4.5.

As it can be observed, there are differences in the values obtained for the diffusion coefficient and Henry's constant for each DES when comparing both experiments. As can be seen in Table 4.5, water content can have a different impact in Henry's constant and diffusion coefficient of a DES depending on its constitution (HBA and HBD used). This can be confirmed as a difference of only 2.44% in water content in ChCl:MA between the first and second solubility test could have had a strong impact in the results as it led to significant rise in Henry's constant (61.41%) and in the diffusion coefficient (95.51%) of this DES. On the contrary to the other ChCl-based DES, ChCl:LA a 60.52% water content difference led only to a 6.70% decrease in Henry's constant and still a high 88.85% difference in the diffusion coefficient. Furthermore, when it comes to the difference in results for the diffusion coefficient of the DES in general, it can be linked to how the diffusion of a gas is affected by viscosity, which is affected by the water present in the DES. A higher water content leads to a decrease in viscosity, which facilitates the diffusion of $CO_2$ through the DES as can be seen by higher values of diffusion coefficient in the second experiment[56]. Consequently , the results obtained from the first experiment were used in order to be possible to compare and analyze the solubility results between DES pre-equilibrated in this salt but also with the same DES pre-equilibrated in the other salt listed in Table 4.6 (magnesium nitrate hexahydrate $a_w$=0.529).

Table 4.5- $CO_2$ Henry's constant and diffusion coefficient for DES pre-equilibrated in $a_w$=0.112.

| DES Sample | Experience | Water content(wt%) | H | D($cm^2s^{-1}$ ) |
|---|---|---|---|---|
| **ChCl:MA** | 1 | 3.76 | 20.00 | $1.1 \times 10^{-8}$ |
| | 2 | 4.47 | 51.83 | $2.45 \times 10^{-7}$ |
| **LA:L-Pro:W** | 1 | 1.93 | 43.50 | $1.09 \times 10^{-8}$ |
| | 2 | 3.37 | 60.00 | $1.06 \times 10^{-7}$ |
| **Gly:L-Pro** | 1 | 1.05 | 20.00 | $8.15 \times 10^{-8}$ |
| | 2 | 1.91 | 37.95 | $1.80 \times 10^{-7}$ |
| **ChCl:LA** | 1 | 1.82 | 59.25 | $4.37 \times 10^{-8}$ |
| | 2 | 4.61 | 55.28 | $3.92 \times 10^{-7}$ |

Table 4.6- Results of $CO_2$ Henry's constant and diffusion coefficient for DES pre-equilibrated in $a_w$=0.529.

| DES Sample | Experience | Water content(wt%) | H | D($cm^2s^{-1}$) |
|---|---|---|---|---|
| **ChCl:MA** | 1 | 12.01 | 20.00 | $4.44 \times 10^{-8}$ |
| **LA:L-Pro:W** | 1 | 9.15 | 57.84 | $3.30 \times 10^{-7}$ |
| **Gly:L-Pro** | 1 | 11.28 | 49.20 | $4.2 \times 10^{-7}$ |
| **ChCl:LA** | 1 | 13.99 | 60.00 | $1.21 \times 10^{-7}$ |

The $CO_2$ diffusion coefficient increases with an increase in the water content, which is related to a decrease in viscosity, which is a property that plays a vital role in the rate of diffusion of $CO_2$ in DES structure, since the lower the viscosity of a DES the easier it is for $CO_2$ molecules to move within the DES structure which translates into a higher diffusion rate[59]. The impact of water on DES viscosity from different $a_w$ is closely linked to this behavior (see Table 4.5 and Table 4.6). For DES at $a_w$=0.112, the higher viscosity values when in comparison with $a_w$=0.529 which are related to lower water content levels, make mass transfer more difficult through its structure, which translates into lower $D_{CO2}$ values for all DES studied. For example, for Gly:L-Pro the water content increases from 1.05 to 11.28wt.% which leads to an increase of the diffusion coefficient from $8.15 \times 10^{-8}$ $cm^2.s^{-1}$ to $4.2 \times 10^{-7}$ $cm^2.s^{-1}$. When in comparison with values found in literature for the studied DES, the ChCl:LA diffusion coefficients obtained for the two water activities ($4.37 \times 10^{-8}$$cm^2.s^{-1}$ and $1.21 \times 10^{-7}$ $cm^2.s^{-1}$) are much lower than the one

obtained by Xin et al.[60] at 25ºC ($0.50 \times 10^{-6}$ $cm^2.s^{-1}$) and at 40ºC ($0.92 \times 10^{-6}$ $cm^2.s^{-1}$) under no pre-equilibrium conditions. Moreover, the diffusion coefficient can also be directly related to the DES local structure and interaction strength between each component[61]. Gly:L-Pro has the highest $CO_2$ diffusion coefficients for both water activities, when compared to the other DES despite having the second highest viscosity for both salts, which can be probably related to the way the interactions between the HBD (glycerol) and the HBA (L-Proline) are formed, which can enhance the diffusion of $CO_2$ molecules through the DES.

In Table 4.5 and Table 4.6 the values obtained for Henry's constant are expressed for each one of the DES without CA. It is known that for a gas, for the same partial pressure, that a lower value of Henry's constant translates into a higher gas solubility[62]. Henry's constant is higher with increasing water content for all DES, except for ChCl:MA and ChCl:LA where no significant change is observed. This trend confirms the results of previous studies that have shown that in some cases a decline in the DES capacity to capture $CO_2$ can result from absorbed water molecules competing with $CO_2$ molecules for absorption sites in DES structure [63]. Among the DES from both salts, ChCl:MA and Gly:L-Pro have the lowest Henry's constant for both conditioning environments, and therefore the highest $CO_2$ solubility. This can possibly be explained in part due to the chemical interaction of the functional groups of the HBDs of these DES with $CO_2$, which also plays a vital role alongside the water content present in each DES. A study on the solubility of $CO_2$ in the eutectic mixture of choline chloride and levulinic acid, also known as furfuryl alcohol, was carried out by Lu *et al* [9]. The researchers concluded that the levulinic acid-based DES are more soluble than the furfuryl alcohol-based DES, which was attributed to the fact that carboxyl groups (–COOH) possess higher affinity for $CO_2$ than the hydroxyl groups (–OH). These conclusions can help explain the lower Henry's constant values for ChCl:MA (20.00 and 20.00) when in comparison to ChCl:LA (59.25 and 60.00). The presence of two carboxyl groups in each molecule of MA when compared to only one carboxyl group in each molecule of LA is a possible explanation for the higher affinity of ChCl:MA for $CO_2$ capture than ChCl:LA. According to literature[9], functional groups of DES interact with $CO_2$ in the following order of strength: amino (-$R_1$(NH)$R_2$)> carbonyl ($R_1$(C=O)$R_2$)> ether ($R_1$-O-$R_2$)> hydroxyl (-OH). Still, it has been also reported that glycerol based DES solubilities are higher than DES with carbonyl groups**.** Three free alcoholic hydroxyl groups are present in glycerol. Because of their strong affinity for $CO_2$ molecules, the hydroxyl groups enhance the absorption of $CO_2$. The high polarity of the bonds in the $CO_2$ molecules allows a strong electron interaction with the highly polar hydroxyl groups in the solvent[64]. Consequently, in Gly:L-Pro (2.5:1),

the presence not only of 3 hydroxyl groups (-OH) per molecule of glycerol but also the presence of an amino group and a carboxylic group in each L-proline molecule enhances DES and $CO_2$ interactions contributing probably to a higher chemical absorption of $CO_2$. Additionally, this outcome is also consistent with the findings of Sarmad *et al.*[65] and Leron *et al.*[66]who showed that solvents based on glycerol had a high capacity for solubilizing $CO_2$.

#### 4.1.1.5 Impact of Carbonic Anhydrase in $CO_2$ diffusivity and Henry's constant

To assess the effect of carbonic anhydrase (CA) in $CO_2$ diffusivity and solubility, solubility tests were also conducted for the same DES at 30ºC with the presence of this enzyme for different $a_w$ values. Table 4.7 shows the results obtained from the experiments carried out for lithium chloride salt ($a_w$=0.112). The results obtained from the first experiment were used to be possible to compare and analyze the solubility results between DES with enzyme pre-equilibrated in this salt but also with the same DES with enzyme pre-equilibrated in the other salt, magnesium nitrate hexahydrate ($a_w$=0.529) with different water content levels listed in Table 4.8. Moreover, this was also the case for the analysis done for the assessment of the impact of CA on DES solubility when compared to DES without CA previously analyzed.

Table 4.7- $CO_2$ Henry's constant and diffusion coefficient for DES with CA pre-equilibrated in $a_w$=0.112.

| DES Sample | Experience | Water content(%wt.) | H | D($cm^2s^{-1}$ ) |
|---|---|---|---|---|
| **ChCl:MA_CA** | 1 | 1.88 | 59.99 | $4.62 \times 10^{-8}$ |
| | 2 | 4.14 | 60.00 | $1.34 \times 10^{-7}$ |
| **LA:L-Pro:W_CA** | 1 | 2.09 | 49.73 | $2.44 \times 10^{-8}$ |
| | 2 | 3.77 | 59.99 | $6.96 \times 10^{-8}$ |
| **Gly:L-Pro_CA** | 1 | 1.62 | 20.00 | $1.27 \times 10^{-8}$ |
| | 2 | 1.70 | 59.99 | $3.02 \times 10^{-8}$ |
| **ChCl:LA_CA** | 1 | 2.50 | 20.00 | $1.05 \times 10^{-8}$ |
| | 2 | 3.60 | 25.49 | $2.31 \times 10^{-7}$ |

Table 4.8- Results of $CO_2$ Henry's constant and diffusion coefficient for DES with CA pre-equilibrated in $a_w$=0.529.

| DES Sample | Experience | Water content(%wt) | H | D($cm^2s^{-1}$) |
|---|---|---|---|---|
| **ChCl:MA_CA** | 1 | 12.23 | 58.51 | $4.44 \times 10^{-8}$ |
| **LA:L-Pro:W_CA** | 1 | 9.15 | 60.00 | $3.30 \times 10^{-7}$ |
| **Gly:L-Pro_CA** | 1 | 11.45 | 22.35 | $4.2 \times 10^{-7}$ |
| **ChCl:LA_CA** | 1 | 14.00 | 42.15 | $1.21 \times 10^{-7}$ |

The $CO_2$ diffusion coefficient once again as for the DES without CA generally increases with the increase of water content (%wt) which is related to the DES viscosity decrease. The exception is ChCl:MA_CA at $a_w$=0.529, in which the diffusion coefficient obtained was lower than expected when in comparison to the same DES with lower water content at $a_w$=0.112. When compared to the DES without CA, it is possible to observe that in the presence of the enzyme, the water content at equilibrium in the DES is different, which can be possibly explained by the alteration of affinity of the DES for water caused by the presence of CA. Furthermore, according to the results the effect of the enzyme is more pronounced in the $CO_2$ diffusion coefficient of the studied DES at lower water content values than for higher water content values, when in comparison with the DES without enzyme.

Table 4.7 and Table 4.8 show the effect of CA in Henry's constant of the DES, and therefore in their $CO_2$ solubility. As it is observed for the DES without CA in Table 4.5 and Table 4.6, Henry's constant is higher with increasing water content for all DES, except for ChCl:MA where a slightly lower value is observed. On the other hand, the presence of CA should help enhance the solubility of DES when comparing with the ones without CA. Nevertheless, it is observed that isn't always confirmed when comparing values of Henry's constant of the same DES pre-equilibrated in the same $a_w$ in the presence and absence of this enzyme (see Table 4.5,Table 4.6,Table 4.7 and Table 4.8). In the presence of CA, for the DES in the lithium chloride salt ($a_w$=0.112) and magnesium nitrate hexahydrate salt ($a_w$=0.529), ChCl:LA has a higher solubility which is translated by a decrease of Henry's constant of the DES with enzyme when compared with the same DES without enzyme. The solubility of Gly:L-Pro is not affected by the presence of the enzyme at a lower water content but for a higher water content , the effect of CA is observed since for $a_w$=0.529 the DES with enzyme has a lower Henry's constant and therefore higher solubility than the DES without enzyme. Since the DESs utilized are

hydrophilic/hygroscopic, in the cases where the solubility decreased in comparison to DES without enzyme (LA:L-Pro:W and ChCl:MA in both $a_w$ in which Henry's constant increased), it is plausible that the amount of water available in in these DES was insufficient for the enzyme's solvation in the DES and to increase conformational liberty and activity[38]. This could account for the enzyme's widespread lack of effect in this DES. In these circumstances, the DES and CA may have competed with one another for water, which could have diminished CA's activity, and therefore its capacity to enhance $CO_2$ solubility.

Based on the results obtained, the DES chosen for the impregnation of a supported liquid membrane to study the potential for $CO_2/CH_4$ separation was Gly:L-Pro pre-equilibrated in lithium chloride salt ($a_w$=0.112). This DES Gly:L-Pro was out of the DES pre-equilirated in both salts, the one that showed the best combination of results in terms of $CO_2$ solubility with the lowest value of Henry's constant obtained (H=20.00) alongside ChCl:MA Gly:L-Pro_CA and ChCl:LA_CA in $a_w$=0.112 and ChCl:MA in $a_w$=0.529 but a higher $CO_2$ diffusion coefficient when compared to the mentioned DES ($D_{CO2}$=$8.15 \times 10^{-8}$ $cm^2.s^{-1}$).

#### 4.1.1.6 Gas permeation tests using a supported liquid membrane (SLMs)

The permeability of $CO_2$ and $CH_4$ in the supported liquid membranes was determined. For each of the two pure gases, separate tests were carried out. The ideal selectivity ($\alpha$) between gases was evaluated using Equation 3.4 to investigate the membrane's capacity to be permeable and selective to each gas. The $CO_2/CH_4$ ideal selectivity as a function of $CO_2$ permeability is shown in Figure 4.10. The line represents the Robeson´s upper bound correlation for $CO_2/CH_4$ separation[67]. This upper bound represents the selectivity values obtained experimentally and published so far and can be used to determine the efficiency of a gas separation process using membranes[5]. If the obtained selectivity of a process is above this upper bound, this means that the results are an improvement in comparison to the works previously published in literature.

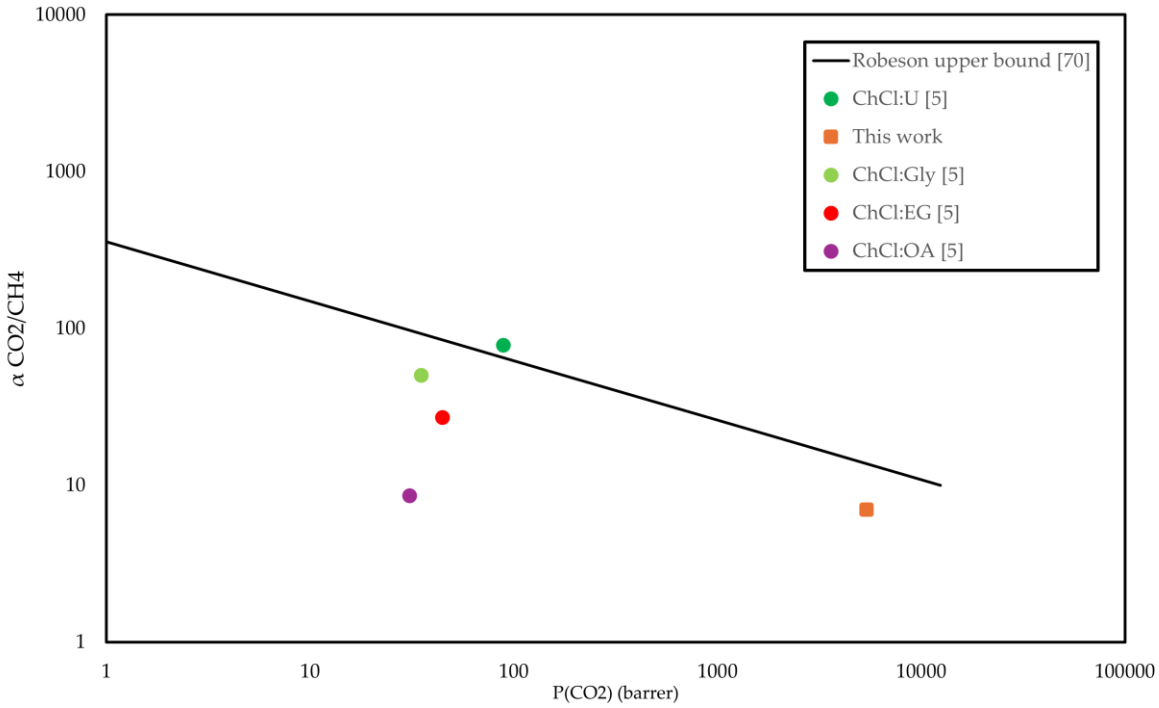


Figure 4.10- $CO_2/CH_4$ selectivity as function of permeability for supported liquid membranes impregnated with DES.

As can be observed in Figure 4.10, the SLM prepared in this work with the DES Gly:L-Pro is the DES that presents the highest $CO_2$ permeability value when compared to other SLMs with DES [7]. Gas permeability(P) accounts for the combined effect of diffusivity and solubility of a gas in the DES that fills the pores of the membrane[7]. Even though $CO_2$ diffusivity is significantly lower for Gly:L-Pro when compared to the other reported DES, the lower value of Henry's constant (H=20.00), which is related to the high affinity for $CO_2$ and a higher solubility capacity of this DES when compared to the other DES is enough to suppress a lower value of diffusion and explain the highest $CO_2$ permeability value obtained (see Table 4.9). Hence, solubility seems to have a greater impact in the transport of $CO_2$ through the SLM in this case, according to the results obtained.

Table 4.9- $CO_2$ diffusion coefficient, Henry's constant and water content(%wt) of DES found in literature and the DES used in this work for gas permeation tests in a SLM.

| DES | D($cm^2s^{-1}$) | H | water content(%wt) | Ref |
|---|---|---|---|---|
| ChCl:U | $2.74 \times 10^{-6}$ | 58.09 | 2.0 | [5] |
| ChCl:Gly | $1.44 \times 10^{-7}$ | 52.55 | 2.0 | [5] |
| ChCl:OA | $3.56 \times 10^{-6}$ | 45.9 | 20 | [5] |
| ChCl:EG | $2.02 \times 10^{-6}$ | 52.03 | 2.5 | [5] |
| Gly:L-Pro | $8.15 \times 10^{-8}$ | 20.00 | 1.05 | This work |

On the other hand, as can also be observed in Figure 4.10 in comparison with the selectivity values for the other supported liquid membranes impregnated with DES found in literature, the membrane impregnated with Gly:L-Pro has the lowest selectivity value despite having a similar selectivity to ChCl:OA, meaning that its separation performance is worse than the SLM's with ChCl:U, ChCl:Gly, and ChCl:EG reported by Craveiro *et.al*.[5]. When combining this low value of selectivity with the high value of permeability measured, it can be justified by the fact that although there is a high rate of $CO_2$ permeation, there is also in comparison a high amount of $CH_4$ that permeates through the supported liquid membrane, when compared to the other values from literature. This can be probably explained by the fact that the presence of strong polar molecules of water in DES could enhance the hydrogen bond affinity for $CO_2$, leading to higher selectivity for $CO_2$ than $CH_4$ depending on the DES used[14]. When comparing the water content (wt%) of the DES used in this work with the water content of DES from literature, the DES used in this work has the lowest amount of water in its structure, which can result in lower affinity enhancement for $CO_2$ when compared to the other DES and therefore explain the low value of selectivity. Moreover, the selectivity obtained falls below the Robson upper bound meaning that this system is less efficient for $CO_2/CH_4$ separation when comparing to the ones reported. This means that membranes impregnated with Gly:L-Pro used in this work have lower potential to be used for $CO_2/CH_4$ separation when in comparison to the systems reported.

# 5 CONCLUSIONS AND FUTURE WORK

## 5.1 Conclusions

The main objective of this work was to evaluate the potential of supported liquid membranes impregnated with DES for biogas upgrading.

To accomplish this, four different DES with and without the presence of enzyme carbonic anhydrase, were tested choline chloride: malonic acid (ChCl:MA), choline chloride: lactic acid (ChCl:LA), lactic acid:l-proline:water (LA:L-Pro:W) and glycerol:l-proline (Gly:L-Pro). DES with different $a_w$ values were also tested (0.112, 0.226, 0.529, 0.843). The prepared DES were characterized in terms of FTIR, viscosity and density, and the $CO_2$ diffusion coefficient and Henry's constant were determined. The obtained results show that the presence of enzyme for the DES with $a_w$=0.112 results in a lower Herny's constant and therefore higher $CO_2$ solubility of ChCl:LA, while at $a_w$=0.529 both ChCl:LA and Gly:L-Pro showed a lower Herny's constant and higher $CO_2$ solubility when compared with the same DES without enzyme. The presence of enzyme carbonic anhydrase is reported to result in a higher $CO_2$ solubility, but this effect was not observed in DES ChCl:LA and Gly:L-Pro with $a_w$=0.529, which can be explained by an insufficient amount of water for the enzyme's solvation in the DES, possibly hindering the enzyme's conformational liberty and optimum activity. The highest solubility value was obtained for DES Gly:L-Pro with $a_w$=0.112, as it obtained the lowest $CO_2$ Henry's constant and also the highest diffusion coefficient value. Considering these results, this DES was chosen to study the potential for $CO_2/CH_4$ separation, using a supported liquid membrane. Gas permeability tests were carried out for $CO_2$ and $CH_4$ mixtures. The DES presented high $CO_2$ permeability and low selectivity when compared to DES reported in literature, probably because the DES used in this work has the lowest amount of water in its structure, which can result in lower affinity enhancement for $CO_2$ when compared to the other DES and therefore explain the low value of selectivity. By determining the selectivity of the prepared SLM, it was possible to evaluate the potential for biogas upgrading and it was concluded that the prepared membrane impregnated with Gly:L-Pro used in this work has lower potential to be used for $CO_2/CH_4$ separation when in comparison to other systems reported.

## 5.2 Future work

The system of a supported liquid membrane impregnated with a DES for biogas upgrading, proposed in this work, resulted in a membrane with a high gas permeability but not as selective for $CO_2$ when comparing to $CH_4$ compared to other DES supported liquid membranes reported in literature, not allowing efficient biogas upgrading of a biogas stream. On the other hand, this work also showed interesting results that need to be further optimized, namely:

- The use of a glycerol-based DES at a low water activity level ($a_w$=0.112) proved to be the system with higher affinity for $CO_2$ out of the ones tested. It is proposed that future work should focus on studying the potential of different types of glycerol-based DES at the same water activity level, to investigate possible improvements in $CO_2$ capture when compared to the one obtained by this system.
- The scale-up of supported liquid membranes impregnated with DES system should be studied to be used as a stage of an industrial biogas upgrading process, to assess its industrial viability.
- Hollow fiber supported liquid membranes should be tested and compared to the flat sheet supported liquid membranes used in this work and compare their efficiency in terms of permeability and selectivity to the results obtained in this work.
- An efficient method to follow the kinetics of the conversion mechanism of $CO_2$ by carbonic anhydrase should be used.
- Efficient methods for DES regeneration should be addressed in order to be possible to lower the amount of DES production needed for biogas purification in case of this system being used at industrial scale.

# 6 REFERENCES


[1] C. Boehringer, "The Kyoto Protocol: A Review and Perspectives," 2019, accessed 15 June 2023, https://www.researchgate.net/publication/23755618.

[2] M. J. B. Kabeyi and O. A. Olanrewaju, "Biogas Production and Applications in the Sustainable Energy Transition," *Journal of Energy*, vol. 2022, pp. 1–43, Jul. 2022, doi: 10.1155/2022/8750221.

[3] B. Bharathiraja, T. Sudharsana, J. Jayamuthunagai, R. Praveenkumar, S. Chozhavendhan, and J. Iyyappan, "Biogas production – A review on composition, fuel properties, feed stock and principles of anaerobic digestion," *Renewable and Sustainable Energy Reviews*, vol. 90. Elsevier Ltd, pp. 570–582, Jul. 01, 2018. doi: 10.1016/j.rser.2018.03.093.

[4] A. Wellinger, "Biogas Upgrading and Utilisation," 2000, accessed 28 May 2023, https://www.researchgate.net/publication/245587554.

[5] R. Craveiro, L. A. Neves, A. R. C. Duarte, and A. Paiva, "Supported liquid membranes based on deep eutectic solvents for gas separation processes," *Sep Purif Technol*, vol. 254, Jan. 2021, doi: 10.1016/j.seppur.2020.117593.

[6] C. Moya, R. Santiago, D. Hospital-Benito, J. Lemus, and J. Palomar, "Design of biogas upgrading processes based on ionic liquids," *Chemical Engineering Journal*, vol. 428, Jan. 2022, doi: 10.1016/j.cej.2021.132103.

[7] L. A. Neves, J. G. Crespo, and I. M. Coelhoso, "Gas permeation studies in supported ionic liquid membranes," *J Memb Sci*, vol. 357, no. 1–2, pp. 160–170, Jul. 2010, doi: 10.1016/j.memsci.2010.04.016.

[8] M. Mubashir, F. N. D'Angelo, and F. Gallucci, "Recent Advances and Challenges of Deep Eutectic Solvent based Supported Liquid Membranes," *Separation and Purification Reviews*, vol. 51, no. 2, pp. 226–244, 2022, doi: 10.1080/15422119.2021.1901742.

[9] I. Cichowska-Kopczyńska, B. Nowosielski, and D. Warmińska, "Deep Eutectic Solvents: Properties and Applications in CO2 Separation," *Molecules*, vol. 28, no. 14. Multidisciplinary Digital Publishing Institute (MDPI), Jul. 01, 2023. doi: 10.3390/molecules28145293.

[10] C. Aravena, D. Lee, J. Park, and Y. Yoo, "Characteristics of Deep eutectic solvents for CO2 capture with Hydro effects for improvement of mass transfer," *Journal of Industrial and Engineering Chemistry*, vol. 111, pp. 337–345, Jul. 2022, doi: 10.1016/j.jiec.2022.04.015.

[11] S. A. Ali *et al.*, "Recent Advances in the Synthesis, Application and Economic Feasibility of Ionic Liquids and Deep Eutectic Solvents for CO2 Capture: A Review," *Energies*, vol. 15, no. 23. MDPI, Dec. 01, 2022. doi: 10.3390/en15239098.

[12] M. Farah, J. Giralt, F. Stüber, J. Font, A. Fabregat, and A. Fortuny, "Supported liquid membranes for the removal of pharmaceuticals from aqueous solutions," *Journal of Water Process Engineering*, vol. 49, Oct. 2022, doi: 10.1016/j.jwpe.2022.103170.

[13] "Biogas: Converting Waste to Energy," 2017, accessed 15 May 2023, www.eesi.org.

[14] T. Quaid and M. T. Reza, "Carbon Capture from Biogas by Deep Eutectic Solvents: A COSMO Study to Evaluate the Effect of Impurities on Solubility and Selectivity," *Clean Technologies*, vol. 3, no. 2, pp. 490–502, Jun. 2021, doi: 10.3390/cleantechnol3020029.

[15] O. W. Awe, Y. Zhao, A. Nzihou, D. P. Minh, and N. Lyczko, "A Review of Biogas Utilisation, Purification and Upgrading Technologies," *Waste and Biomass Valorization*, vol. 8, no. 2. Springer Science and Business Media B.V., pp. 267–283, Mar. 01, 2017. doi: 10.1007/s12649-016-9826-4.

[16] M. Calero, V. Godoy, C. G. Heras, E. Lozano, S. Arjandas, and M. A. Martín-Lara, "Current state of biogas and biomethane production and its implications for Spain," *Sustainable Energy and Fuels*, vol. 7, no. 15. Royal Society of Chemistry, pp. 3584–3602, Jun. 05, 2023. doi: 10.1039/d3se00419h.

[17] P. S. Domingues, "Main Biogas Upgrading Technologies," *International Journal of Environmental Sciences & Natural Resources*, vol. 27, no. 4, Apr. 2021, doi: 10.19080/ijesnr.2021.27.556219.

[18] "Tracking biogas and biomethane deployment across Europe.", *European Biogas Association Statistical Report 2022.*

[19] "A Gas for Climate report Feasibility of REPowerEU 2030 targets, production potentials in the Member Biomethane production potentials in the EU," 2022, accessed 1 July 2023, https://gasforclimate2050.eu/.

[20] P. Sulewski, W. Ignaciuk, M. Szymańska, and A. Wąs, "Development of the Biomethane Market in Europe," *Energies*, vol. 16, no. 4. MDPI, Feb. 01, 2023. doi: 10.3390/en16042001.

[21] C. Moya, R. Santiago, D. Hospital-Benito, J. Lemus, and J. Palomar, "Design of biogas upgrading processes based on ionic liquids," *Chemical Engineering Journal*, vol. 428, Jan. 2022, doi: 10.1016/j.cej.2021.132103.

[22] C. Soto, L. Palacio, R. Muñoz, P. Prádanos, and A. Hernandez, "Recent Advances in Membrane-Based Biogas and Biohydrogen Upgrading," *Processes*, vol. 10, no. 10. MDPI, Oct. 01, 2022. doi: 10.3390/pr10101918.

[23] C. A. Grande, "Advances in Pressure Swing Adsorption for Gas Separation," *ISRN Chemical Engineering*, vol. 2012, pp. 1–13, Dec. 2012, doi: 10.5402/2012/982934.

[24] J. Niesner, D. Jecha, and P. Stehlík, "Biogas upgrading technologies: State of art review in european region," in *Chemical Engineering Transactions*, Italian Association of Chemical Engineering - AIDIC, 2013, pp. 517–522. doi: 10.3303/CET1335086.

[25] M. Wang, A. Lawal, P. Stephenson, J. Sidders, and C. Ramshaw, "Post-combustion CO2 capture with chemical absorption: A state-of-the-art review," *Chemical Engineering Research and Design*, vol. 89, no. 9, pp. 1609–1624, Sep. 2011, doi: 10.1016/j.cherd.2010.11.005.

[26] F. A. Chowdhury, H. Yamada, T. Higashii, K. Goto, and M. Onoda, "CO2 capture by tertiary amine absorbents: A performance comparison study," *Ind Eng Chem Res*, vol. 52, no. 24, pp. 8323–8331, Jun. 2013, doi: 10.1021/ie400825u.

[27] A. Prabhune and R. Dey, "Green and sustainable solvents of the future: Deep eutectic solvents," *J Mol Liq*, vol. 379, Jun. 2023, doi: 10.1016/j.molliq.2023.121676.

[28] R. L. Vekariya, "A review of ionic liquids: Applications towards catalytic organic transformations," *Journal of Molecular Liquids*, vol. 227. Elsevier B.V., p. 44, Feb. 01, 2017. doi: 10.1016/j.molliq.2016.11.123.

[29] F. U. Shah, R. An, and N. Muhammad, "Editorial: Properties and Applications of Ionic Liquids in Energy and Environmental Science," *Frontiers in Chemistry*, vol. 8. Frontiers Media S.A., Dec. 15, 2020. doi: 10.3389/fchem.2020.627213.

[30] B. B. Hansen *et al.*, "Deep Eutectic Solvents: A Review of Fundamentals and Applications," 2020.

[31] K. Xin, I. Roghair, F. Gallucci, and M. van Sint Annaland, "Total vapor pressure of hydrophobic deep eutectic solvents: Experiments and modelling," *J Mol Liq*, vol. 325, Mar. 2021, doi: 10.1016/j.molliq.2020.115227.

[32] I. Cichowska-Kopczyńska, D. Warmińska, and B. Nowosielski, "Solubility of carbon dioxide in deep eutectic solvents based on 3-amino-1-propanol and tetraalkylammonium

salts at low pressure," *Materials*, vol. 14, no. 3, pp. 1–14, Feb. 2021, doi: 10.3390/ma14030594.

[33] T. Marino and A. Figol, "Arsenic removal by liquid membranes," *Membranes*, vol. 5, no. 2. MDPI AG, pp. 150–167, Mar. 27, 2015. doi: 10.3390/membranes5020150.

[34] A. Nogalska, A. Trojanowska, and R. Garcia-Valls, "Membrane contactors for CO2 capture processes - Critical review," *Physical Sciences Reviews*, vol. 2, no. 7, Jul. 2019, doi: 10.1515/psr-2017-0059.

[35] M. Khajenoori and M. Asghari, "MASS TRANSFER IN HOLLOW FIBER GAS-LIQUID MEMBRANE CONTACTORS FOR ACID GAS CAPTURE: A REVIEW.",2021, accessed 4th September, www.SID.ir.

[36] M. Li *et al.*, "Removal of CO2 from biogas by membrane contactor using PTFE hollow fibers with smaller diameter," *J Memb Sci*, vol. 627, Jun. 2021, doi: 10.1016/j.memsci.2021.119232.

[37] G. B. Smejkal and S. Kakumanu, "Enzymes and their turnover numbers," *Expert Review of Proteomics*, vol. 16, no. 7. Taylor and Francis Ltd, pp. 543–544, Jul. 03, 2019. doi: 10.1080/14789450.2019.1630275.

[38] L. A. Neves, C. Afonso, I. M. Coelhoso, and J. G. Crespo, "Integrated CO 2 capture and enzymatic bioconversion in supported ionic liquid membranes," in *Separation and Purification Technology*, Sep. 2012, pp. 34–41. doi: 10.1016/j.seppur.2012.01.049.

[39] C. D. Boone, S. Gill, A. Habibzadegan, and R. McKenna, "Carbonic anhydrase: An efficient enzyme with possible global implications," *International Journal of Chemical Engineering*. 2013. doi: 10.1155/2013/813931.

[40] R. Fortunato *et al.*, "Liquid membranes using ionic liquids: The influence of water on solute transport," *J Memb Sci*, vol. 249, no. 1–2, pp. 153–162, Mar. 2005, doi: 10.1016/j.memsci.2004.10.007.

[41] L. Greenspan, "Humidity Fixed Points of Binary Saturated Aqueous Solutions.", JOURNAL OF RESEARCH of the National Bureau of Standards - A. Physics and ChemistryVol. 81 A, No.1, January- February 1977.

[42] H. Tiernan, B. Byrne, and S. G. Kazarian, "ATR-FTIR spectroscopy and spectroscopic imaging for the analysis of biopharmaceuticals," *Spectrochimica Acta - Part A: Molecular and Biomolecular Spectroscopy*, vol. 241. Elsevier B.V., Nov. 05, 2020. doi: 10.1016/j.saa.2020.118636.

[43] R. Verma, "Introduction to Fourier Transform Infrared Spectrometry Introduction to FTIR", doi: 10.13140/RG.2.2.21043.71206.

[44] A. Fadlelmoula, D. Pinho, V. H. Carvalho, S. O. Catarino, and G. Minas, "Fourier Transform Infrared (FTIR) Spectroscopy to Analyse Human Blood over the Last 20 Years: A Review towards Lab-on-a-Chip Devices," *Micromachines*, vol. 13, no. 2. MDPI, Feb. 01, 2022. doi: 10.3390/mi13020187.

[45] T. Miri, "Viscosity and Oscillatory Rheology," in *Practical Food Rheology: An Interpretive Approach*, Wiley-Blackwell, 2010, pp. 7–28. doi: 10.1002/9781444391060.ch2.

[46] G. García, S. Aparicio, R. Ullah, and M. Atilhan, "Deep eutectic solvents: Physicochemical properties and gas separation applications," *Energy and Fuels*, vol. 29, no. 4, pp. 2616–2644, Apr. 2015, doi: 10.1021/ef5028873.

[47] G. M. Thorat, H. S. Jadhav, A. Roy, W. J. Chung, and J. G. Seo, "Dual Role of Deep Eutectic Solvent as a Solvent and Template for the Synthesis of Octahedral Cobalt Vanadate for an Oxygen Evolution Reaction," *ACS Sustain Chem Eng*, vol. 6, no. 12, pp. 16255–16266, Dec. 2018, doi: 10.1021/acssuschemeng.8b03119.

[48] S. Zhang *et al.*, "Carbonic Anhydrase Enzyme-MOFs Composite with a Superior Catalytic Performance to Promote CO 2 Absorption into Tertiary Amine Solution," *Environ Sci Technol*, vol. 52, no. 21, pp. 12708–12716, Nov. 2018, doi: 10.1021/acs.est.8b04671.

[49] C. L. Yiin, K. L. Yap, B. L. Fui Chin, and S. S. Mun Lock, "Insights into the Lignin Dissolution Mechanism of Water Content Tailored-choline Chloride (ChCl) Based Green Solvents for Biomass Pretreatment," *Physical Chemistry Research*, vol. 11, no. 3, pp. 605–614, Sep. 2023, doi: 10.22036/pcr.2022.350557.2131.

[50] S. Chen, Q. An, H. Sun, and M. Mao, "Application of ultrasound-assisted deep eutectic solvent extraction combined with liquid-liquid extraction method to the extraction of three pesticide residues from fruit and vegetable samples," *Acta Chromatogr*, vol. 33, no. 1, pp. 30–36, Mar. 2021, doi: 10.1556/1326.2020.00727.

[51] M. A. Karadendrou, I. Kostopoulou, V. Kakokefalou, A. Tzani, and A. Detsi, "L-Proline-Based Natural Deep Eutectic Solvents as Efficient Solvents and Catalysts for the Ultrasound-Assisted Synthesis of Aurones via Knoevenagel Condensation," *Catalysts*, vol. 12, no. 3, Mar. 2022, doi: 10.3390/catal12030249.

[52] M. S. C. Zain, J. X. Yeoh, S. Y. Lee, and K. Shaari, "Physicochemical properties of choline chloride-based natural deep eutectic solvents (Nades) and their applicability for

extracting oil palm flavonoids," *Sustainability (Switzerland)*, vol. 13, no. 23, Dec. 2021, doi: 10.3390/su132312981.

[53] G. Gygli, X. Xu, and J. Pleiss, "Meta-analysis of viscosity of aqueous deep eutectic solvents and their components," *Sci Rep*, vol. 10, no. 1, Dec. 2020, doi: 10.1038/s41598-020-78101-y.

[54] C. Florindo, F. S. Oliveira, L. P. N. Rebelo, A. M. Fernandes, and I. M. Marrucho, "Insights into the synthesis and properties of deep eutectic solvents based on cholinium chloride and carboxylic acids," *ACS Sustain Chem Eng*, vol. 2, no. 10, pp. 2416–2425, Oct. 2014, doi: 10.1021/sc500439w.

[55] E. L. Smith, A. P. Abbott, and K. S. Ryder, "Deep Eutectic Solvents (DESs) and Their Applications," *Chemical Reviews*, vol. 114, no. 21. American Chemical Society, pp. 11060–11082, Nov. 12, 2014. doi: 10.1021/cr300162p.

[56] A. K. Halder, R. Haghbakhsh, I. V. Voroshylova, A. R. C. Duarte, and M. N. D. S. Cordeiro, "Density of deep eutectic solvents: The path forward cheminformatics-driven reliable predictions for mixtures," *Molecules*, vol. 26, no. 19, Oct. 2021, doi: 10.3390/molecules26195779.

[57] F. G. Calvo-Flores and C. Mingorance-Sánchez, "Deep Eutectic Solvents and Multicomponent Reactions: Two Convergent Items to Green Chemistry Strategies," *ChemistryOpen*, vol. 10, no. 8. John Wiley and Sons Inc, pp. 815–829, Aug. 01, 2021. doi: 10.1002/open.202100137.

[58] V. Bušić, M. Molnar, V. Tomičić, D. Božanović, I. Jerković, and D. Gašo-Sokač, "Choline Chloride-Based Deep Eutectic Solvents as Green Effective Medium for Quaternization Reactions," *Molecules*, vol. 27, no. 21, Nov. 2022, doi: 10.3390/molecules27217429.

[59] H. C. Price *et al.*, "Quantifying water diffusion in high-viscosity and glassy aqueous solutions using a raman isotope tracer method," *Atmos Chem Phys*, vol. 14, no. 8, pp. 3817–3830, Apr. 2014, doi: 10.5194/acp-14-3817-2014.

[60] K. Xin and M. van Sint Annaland, "Diffusivities and solubilities of carbon dioxide in deep eutectic solvents," *Sep Purif Technol*, vol. 307, Feb. 2023, doi: 10.1016/j.seppur.2022.122779.

[61] S. J. Rukmani, B. W. Doherty, O. Acevedo, and C. M. Colina, "Molecular Simulations of Deep Eutectic Solvents: A Perspective on Structure, Dynamics, and Physical Properties.", Reviews in Computational Chemistry Reviews in Computational Chemistry, vol. 32, May. 2022, p. 135-216, doi: https://doi.org/10.1002/9781119625933.ch4

[62] Y. H. Li, W. Zhang, L. Wang, F. H. Zhao, W. Han, and G. C. Chen, "Henry's Law and accumulation of crust-derived helium: A case from Weihe Basin, China," *Natural Gas Geoscience*, vol. 28, no. 4, pp. 495–501, Apr. 2017, doi: 10.11764/j.issn.1672-1926.2017.02.015.

[63] Y. Marcus, "Gas solubilities in deep eutectic solvents," *Monatshefte fur Chemie*, vol. 149, no. 2. Springer-Verlag Wien, pp. 211–217, Feb. 01, 2018. doi: 10.1007/s00706-017-2031-8.

[64] M. J. Aguilar, "Cite this article: Aguilar MJ (2020) Aqueous Solutions of Glycerol and Urine for CO2 Capture," *JSM Environ Sci Ecol*, vol. 8, no. 1, p. 1066, 2020.

[65] S. Sarmad, Y. Xie, J.-P. Mikkola, and X. Ji, "Screening of deep eutectic solvents (DESs) as green CO 2 sorbents: from solubility to viscosity," *New Journal of Chemistry*, vol. 41, no. 1, pp. 290–301, 2017, doi: 10.1039/C6NJ03140D.

[66] R. B. Leron and M. H. Li, "Solubility of carbon dioxide in a eutectic mixture of choline chloride and glycerol at moderate pressures," *J Chem Thermodyn*, vol. 57, pp. 131–136, Feb. 2013, doi: 10.1016/J.JCT.2012.08.025.

[67] L. M. Robeson, "The upper bound revisited," *J Memb Sci*, vol. 320, no. 1–2, pp. 390–400, Jul. 2008, doi: 10.1016/j.memsci.2008.04.030.

# A

# APENDIX